COPERNICUS
MARINE ENVIRONMENT MONITORING SERVICE

QUALITY INFORMATION DOCUMENT

Sea Level TAC - DUACS products:

SEALEVEL_ARC_PHY_L3_NRT_OBSERVATIONS_008_038
SEALEVEL_BS_PHY_L3_NRT_OBSERVATIONS_008_039
SEALEVEL_BS_PHY_L3_REP_OBSERVATIONS_008_040
SEALEVEL_BS_PHY_L4_NRT_OBSERVATIONS_008_041
SEALEVEL_BS_PHY_L4_REP_OBSERVATIONS_008_042
SEALEVEL_EUR_PHY_ASSIM_L3_NRT_OBSERVATIONS_008_043
SEALEVEL_GLO_PHY_L3_NRT_OBSERVATIONS_008_044
SEALEVEL_GLO_PHY_L3_REP_OBSERVATIONS_008_045
SEALEVEL_GLO_PHY_L4_NRT_OBSERVATIONS_008_046
SEALEVEL_GLO_PHY_L4_REP_OBSERVATIONS_008_047
SEALEVEL_MED_PHY_ASSIM_L3_NRT_OBSERVATIONS_008_048
SEALEVEL_MED_PHY_L3_REP_OBSERVATIONS_008_049
SEALEVEL_MED_PHY_L4_NRT_OBSERVATIONS_008_050
SEALEVEL_MED_PHY_L4_REP_OBSERVATIONS_008_051
SEALEVEL_GLO_NOISE_L4_NRT_OBSERVATIONS_008_032
SEALEVEL_GLO_NOISE_L4_REP_OBSERVATIONS_008_033

Issue: 1.3

Contributors: M.-I. Pujol, SL-TAC team.

Approval date by the CMEMS product quality coordination team: **10/07/2017**

CHANGE RECORD

When the quality of the products changes, the QuID is updated and a row is added to this table. The third column specifies which sections or sub-sections have been updated. The fourth column should mention the version of the product to which the change applies.

Issue	Date	§	Description of Change	Author	Validated By
1.0	18/01/2017	all	upgrade for CMEMS V3 upgrade for introduction of Sentinel-3A	M-I. Pujol	A. Melet
1.1	17/03/2017	all	Changes following Mercator review	M-I Pujol	
1.2	31/03/2017	I.1.2 V.4	add validation results	G. Taburet	
1.3	25/04/2017	I.1.1	Changes following Eumetsat review	M-I. Pujol	
1.4	19/06/2017	I.1.3 II.4.5	Upgrade for REP product extension: Introduction of Sentinel-3A, Jason-2 Interleaved Change of Cryosat-2 orbit standard from CPP to GOP	G. Taburet	

TABLE OF CONTENTS

I EXECUTIVE SUMMARY

I.1 Products covered by this document

This document describe the quality of the operational (NRT) and reprocessed (REP/DT) DUACS products listed here after:

I.1.1 Operational products

I.1.1.1 Along-track products

product	SEALEVEL_ARC_PHY_L3_NRT_OBSERVATIONS_008_038
Area	Arctic
satellites	Jason-3; Sentinel-3A, OSTM/Jason-2 interleaved;SARAL-DP/AltiKa; Cryosat-2
Spatial resolution	Along-track 14 km
Temporal resolution	10 days to more than 30 days (variable with satellite) ; products are stored in 1-day files.

product	SEALEVEL_BS_PHY_L3_NRT_OBSERVATIONS_008_039
Area	Black Sea
satellites	Jason-3; Sentinel-3A, OSTM/Jason-2 interleaved;SARAL-DP/AltiKa; Cryosat-2
Spatial resolution	Along-track 7km (full 1Hz resolution)
Temporal resolution	10 days to more than 30 days (variable with satellite) ; products are stored in 1-day files.

product	SEALEVEL_EUR_PHY_ASSIM_L3_NRT_OBSERVATIONS_008_043
Area	Europe
satellites	Jason-3; Sentinel-3A, OSTM/Jason-2 interleaved;SARAL-DP/AltiKa; Cryosat-2
Spatial resolution	Along-track 7km (full 1Hz resolution)
Temporal resolution	10 days to 29 days (variable with satellite) ; products are stored in 1-day files.

product	SEALEVEL_GLO_PHY_L3_NRT_OBSERVATIONS_008_044
Area	Global ocean
satellites	Jason-3; Sentinel-3A, OSTM/Jason-2 interleaved;SARAL-DP/AltiKa; Cryosat-2
Spatial resolution	Along-track 14km
Temporal resolution	10 days to more than 30 days (variable with satellite); products are stored in 1-day files.

product	SEALEVEL_MED_PHY_ASSIM_L3_NRT_OBSERVATIONS_008_048
Area	Mediterranean Sea
satellites	Jason-3; Sentinel-3A, OSTM/Jason-2 interleaved;SARAL-DP/AltiKa; Cryosat-2
Spatial resolution	Along-track 7 km (full 1Hz resolution)
Temporal resolution	10 days to more than 30 days (variable with satellite) ; products are stored in 1-day files.

I.1.1.2 Gridded products

product	SEALEVEL_BS_PHY_L4_NRT_OBSERVATIONS_008_041
Area	Black Sea
satellites	Merging of the different altimeter measurements available
Spatial resolution	1/8°x1/8° Cartesian grid
Temporal resolution	1 day

product	SEALEVEL_GLO_PHY_L4_NRT_OBSERVATIONS_008_046
Area	Global ocean
satellites	Merging of the different altimeter measurements available
Spatial resolution	1/4°x1/4° Cartesian grid
Temporal resolution	1 day

product	SEALEVEL_MED_PHY_L4_NRT_OBSERVATIONS_008_050
Area	Mediterranean Sea
satellites	Merging of the different altimeter measurements available
Spatial resolution	1/8°x1/8° Cartesian grid
Temporal resolution	1 day

I.1.2 Reanalysis products

The reanalysis products covered by this document cover the period from 1993. The dataset is regularly completed with a nearly 6-month delay. The different production events of the reanalysis products are listed in §V.4.

I.1.2.1 Along-track products

product	SEALEVEL_BS_PHY_L3_REP_OBSERVATIONS_008_040
Area	Black Sea
satellites	Topex-Poseidon; Topex-Poseidon (interleaved orbit); Jason-1; Jason-1 (interleaved orbit); Jason-1 (geodetic orbit); OSTM/Jason-2; OSTM/Jason-2 (interleaved) ; Jason-3; Sentinel-3A; ERS-1; ERS-2, Envisat; Envisat (extended phase); Geosat Follow On; Cryosat; SARAL/AltiKa, SARAL-DP/ALtiKa; HY-2A, HY-2A geodetic orbit
Spatial resolution	Along-track 7km for filtered and unfiltered
Temporal resolution	10 days to 35 days (variable with satellite) ; products are stored in 1-day files.

product	SEALEVEL_GLO_PHY_L3_REP_OBSERVATIONS_008_045
Area	Global ocean
satellites	Topex-Poseidon; Topex-Poseidon (interleaved orbit); Jason-1; Jason-1 (interleaved orbit); Jason-1 (geodetic orbit); OSTM/Jason-2; OSTM/Jason-2 (interleaved) ; Jason-3; Sentinel-3A; ERS-1; ERS-2, Envisat; Envisat (extended phase); Geosat Follow On; Cryosat; SARAL/AltiKa, SARAL-DP/ALtiKa; HY-2A, HY-2A geodetic orbit
Spatial resolution	Along-track 14km for filtered, 7km for unfiltered
Temporal resolution	10 days to 35 days (variable with satellite) ; products are stored in 1-day files.

product	SEALEVEL_MED_PHY_L3_REP_OBSERVATIONS_008_049
Area	Mediterranean Sea
satellites	Topex-Poseidon; Topex-Poseidon (interleaved orbit); Jason-1; Jason-1 (interleaved orbit); Jason-1 (geodetic orbit); OSTM/Jason-2; OSTM/Jason-2 (interleaved) ; Jason-3; Sentinel-3A; ERS-1; ERS-2, Envisat; Envisat (extended phase); Geosat Follow On; Cryosat; SARAL/AltiKa, SARAL-DP/ALtiKa; HY-2A, HY-2A geodetic orbit
Spatial resolution	Along-track 14km for filtered, 7km for unfiltered
Temporal resolution	10 days to 35 days (variable with satellite) ; products are stored in 1-day files.

I.1.2.2 Gridded products

product	SEALEVEL_BS_PHY_L4_REP_OBSERVATIONS_008_042
Area	Black Sea
satellites	Merging of the different altimeter measurements available
Spatial resolution	1/8°x1/8° Cartesian grid
Temporal resolution	1 day

product	SEALEVEL_GLO_PHY_L4_REP_OBSERVATIONS_008_047
Area	Global ocean
satellites	Merging of the different altimeter measurements available
Spatial resolution	1/4°x1/4° Cartesian grid
Temporal resolution	1 day

product	SEALEVEL_MED_PHY_L4_REP_OBSERVATIONS_008_051
Area	Mediterranean Sea
satellites	Merging of the different altimeter measurements available
Spatial resolution	1/8°x1/8° Cartesian grid
Temporal resolution	1 day

I.1.3 Time invariant Products

product	SEALEVEL_GLO_NOISE_L4_NRT_OBSERVATIONS_008_032 And SEALEVEL_GLO_NOISE_L4_REP_OBSERVATIONS_008_033
Area	Global
satellites	Topex-Poseidon; Topex-Poseidon (interleaved orbit); Jason-1; Jason-1 (interleaved orbit); Jason-1 (geodetic orbit); OSTM/Jason-2; OSTM/Jason-2 (interleaved) ; Jason-3; Sentinel-3A; ERS-1; ERS-2, Envisat; Envisat (extended phase); Geosat Follow On; Cryosat; SARAL/AltiKa, SARAL-DP/ALtiKa; HY-2A, HY-2A geodetic orbit
Spatial resolution	Grid 2°x2°
Temporal resolution	Static

The number of altimeter data processed by the system varies with time, according to satellites availability. The following table summarizes the periods during which the different datasets are available. **Figure 4** shows the different periods during which from 1 up to 4 altimeters were available.

	Temporal availability	
	Begin date	**End date**
merged	NRT : 2017/04/13 REP : 1993/01/01	NRT : y/m* REP : nearly 6-month delay compared to NRT
j3	NRT : 2017/03/28 REP : 2016/06/25	NRT : y/m* REP :nearly 6-month delay compared to NRT *
s3a	NRT : 2017/03/28 REP : 2016/12/26	NRT : y/m* REP :nearly 6-month delay compared to NRT
al	NRT : 2017/03/28 REP :2013/03/14	NRT : y/m* REP :2016/07/04
alg	NRT : see al REP :2016/07/04	NRT : see al REP :nearly 6-month delay compared to NRT *
j2	NRT : no more processed REP :2008/10/19 (REP)	NRT : no more processed REP : 2016/06/25
j2n	NRT : 2017/03/28 REP : 2016/10/17	NRT : y/m* REP : nearly 6-month delay compared to NRT
c2	NRT : 2017/03/28 REP :2011/01/28	NRT : y/m * REP :nearly 6-month delay compared to NRT *
h2	REP :2014/03/12	REP :2016/03/15
h2g	REP : not yet processed	REP : not yet processed
j1g	REP :2012/05/07	REP :2013/06/21
j1n	REP :2009/02/14	REP :2012/03/03
j1	REP :2002/04/24	REP :2008/10/19
g2	REP :2000/01/07	REP :2008/09/07
enn	REP :2010/10/26	REP :2012/04/08
en	REP :2002/10/08	REP :2010/10/21
e1**	REP :1993/01/01	REP :1995/05/15
e2	REP :1995/05/15	REP :2002/10/08
tpn	REP :2002/09/16	REP :2005/10/08
tp	REP :1992/09/25	REP :2002/04/24

*: those dates are updated regularly (3 to 4 times per year for REP; daily for NRT)

**: ERS-1: Geodetic phases (E-F) are included. No ERS-1 data between December 23,1993 and April 10, 1994 (ERS-1 phase D - 2nd ice phase).

Table 1: Temporal period processed by DUACS for the different products/datasets.

I.2 Summary of the results

The quality of the REP/DT DUACS products as been assessed by comparison with independent measurements (in situ and satellite) and in coordination with other projects (ESA SL_cci and CNES SALP). The NRT products are assessed by routine validation and in comparison with REP/DT products. The results are summarized below.

SLA and ADT :

The sea level long-term/climatic trend signal can be monitored with DT/REP products. The errors have been estimated to be lower than 0.5mm/yr at global scale, and lower than 3mm/yr at regional scale. NRT products should not been used for such long-term signal analysis due to frequent constellation/platforms events that can induce jumps/discontinuities/drifts in the time series.

Sea level Errors for mesoscalesvary between 1.4 cm² in low variability areas to more than 30 cm² in high variability areas. This estimation is based on a 2-satellite constellation in DT conditions. Errors observed on gridded L4 products are expected to be reduced when additional altimeters are available. NRT products quality is reduced due to the unavailability of altimeter measurements in the future. 4 altimeters are required in NRT conditions to reach the 2-altimeter DT capabilities. Wavelengths accessible with gridded products are larger than nearly 180km.

Along-track SLA/ADT fields also include residual noise measurements (uncorrelated) errors that are spatiallyand temporally variable (correlation with wave heights) and differ from an altimeter to the other. Characteristic mean noise values over the global ocean vary between 2-4 cm rms for raw measurement and 0.7-1.3 cm for filtered products. The presence of this noise measurement limits the observability of the wavelengths shorter than ~65km (global mean value).

Geostrophic currents:

Geostrophic currents derived from altimeter gridded products are usually underestimated when compared to the in-situ observations. Errors on geostrophic currents have been estimated to range between 5 and 15 cm/s depending on the ocean surface variability. As for SLA field, NRT products quality is reduced and more sensitive to the constellation changes.

System version changes:

The CMEMS V3.0 version of the NRT DUACS products includes measurements from 5 different altimeters: Jason-3, OSTM/Jason-2 interleaved, SARAL-DP/AltiKa, Cryosat-2 and Sentinel-3A. The quality of the DUACS products strongly depends on the quality of the L2 products used asinput of the processing. During the last months, different events have had an impact on the DUACS products quality:

- Availability of new altimeters: early 2016 Jason-3 and Sentinel-3A altimeters were launched. DUACS introduced these L2P measurements as soon as available. Jason-3 was introduced in September 2016 as the new reference mission; Sentinel -3A was introduced in April 2017 as a complementary mission.
- Additionally, different altimeters were positioned on a new orbit during year 2016: HY-A was moved on a geodetic orbit in March 2016; SARAL/AltiKa was moved on a drifting orbit in July 2016; OSTM/Jason-2 was moved on an interleaved orbit on September 2016. During each orbit maneuver, the data availability was reduced or interrupted for a few days.
- Finally, DUACS implemented new version of the system in order to improve the product quality: in April 2017, new variables were introduced in the DUACS products. They consist in Absolute Dynamic Topography (L3 and L4) and geostrophic current (L4). Additionally, a new Mean Sea Surface solution was used for the Arctic product generation, increasing the product quality over this area.

As done in NRT processing, the different constellation changes are/will be implemented in DT processing as soon as GDR/NTC products are available.

I.3 Estimated Accuracy Numbers

The EAN are representative of the signature of different error signals on the products, including both uncorrelated (i.e. noises) and correlated (spatial and temporal scales) error signals.

Noise measurement:

The noise measurement error (i.e. uncorrelated error) was specifically estimated at regional scale. It is presented in §IV.1.1.2.1. A Synthesis is given inTable 2.

	Global Ocean	**Mediterranean and Black Sea**	**Europe (excluding Med and Black Sea)**
Sentinel-3A	**2.4** (0.9)	To be defined	To be defined
Jason-3	**2.9** (1.1)	**2.4** (0.95)	**2.9** (1.63)
Jason-2	**2.9** (1.1)	**2.4** (0.95)	**2.9** (1.63)
Cryosat-2	**2.5** (1.0)	**2.1** (0.84)	**2.6** (1.45)
SARAL/AltiKa	**2.1** (0.8)	**1.75** (0.71)	**2.2** (1.21)
HY-2A	**3.1** (1.2)	**2.5** (0.71)	**-**
Topex/Poseidon	**2.9** (1.1)	**1.9** (0.78)	**-**
Jason-1	**2.9** (1.1)	**2.4** (0.94)	-
Envisat	**2.5** (1.0)	**2.0** (0.81)	-
ERS-1	**3.5** (1.3)	**2.9** (1.15)	-
ERS-2	**3.8** (1.4)	**3.1** (1.24)	-
Geosat Follow On	**3.2** (1.3)	**2.7** (1.06)	**-**

Table 2: Mean 1Hz noise measurement observed for the different altimeters on along-track (L3) DUACS products. Noise for raw measurement (bold) and filtered (low-pass filtering; cut-off 65km) SLA (parenthesis) are indicated. Unit: cm rms.

MSL trend & climatic scales:

The errors at climatic scales were estimated within the ESA SL_cci project (see §IV.1.1.2.2; synthesis given in Table 3)

Spatial scales	**Temporal scales**	**Altimetry errors**
Global MSL	Long-term evolution (> 10 years)	< 0.5 mm/yr
	Interannual signals (< 5 years)	< 2 mm over 1 year
	Annual signals	< 1 mm
Regional MSL	Long term evolution (> 10 years)	< 3 mm/yr
	Annual signals	< 10mm

Table 3: Estimated errors at climatic scales observed on SLA DUACS reanalysis products (L3 & L4). (from Ablain et al, 2015)

Mesoscale:

For merged maps (L4 products), EAN were estimated using the results of comparisons between maps and independent along-track data. They represent a degraded version of the reprocessed product quality. Indeed, they were estimated considering a 2-altimeter constellation available for the merged gridded product computation. Results are summarized in Table 4. A full description is given in Pujol et al (2016) (see also §IV.1.2.2).

	TP [2003-2004]
Reference area*	1.4 (-0.7%)
Dist coast > 200km & variance < 200 cm²	4.9 (-2.1%)
Dist coast > 200km & variance > 200 cm²	32.5 (-9.9%)
Dist coast < 200km	8.9 (-4.1%)

**The reference area is defined by [330,360°E]; [-22,-8°N]*

Table 4: Variance of the differences between gridded (L4) DT2014 two-sat-merged products and independent TP interleaved along-track measurements for different geographic selections (unit = cm²). In parenthesis: variance reduction (in %) compared with the results obtained with the DT2010 products. Statistics are presented for wavelengths ranging between 65-500 km and after latitude selection (|LAT| < 60°). (Pujol et al., 2016)

Geostrophic current:

EAN on geostrophic current are deduced from comparison between altimeter L4 products and drifter measurements (see Pujol et al 2016 for methodology). Synthesis is presented in Table 5 (see also §IV.3).

Selection criteria	**zonal**	**meridional**
Global excluding equatorial band	9.6	9.6
High variability areas	15	15
Low variability areas	5.5	5

Table 5: RMS of the differences between DUACS DT2014 geostrophic current (L4) products and independent drifter measurements (unit = cm/s).

Observable wavelengths:

The along-track (L3) and gridded (L4) products are respectively delivered with a 1Hz (not subsampled) and 1/4° for global and 1/8° for regional products. Nevertheless, this spatial sampling is not representative of the effective spatial resolution of the products. Along-track product are affected by measurement noises that limit the observation of the small scales as discussed in §IV.1.1.2.1. Gridded products resolution capability is directly linked to the altimeter constellation state and mapping methodology as discussed in §IV.1.2.2. The effective resolution capability of the products is summarized in Table 6.

	L3 products	**L4 global products**
Wavelengths observable (km)	> ~65	> ~180

Table 6: Effective mean spatial resolution of the DUACS products (L3 & L4) over global ocean

II PRODUCTION SYSTEM DESCRIPTION

II.1 Production center name

SL-CLS-TOULOUSE-FR

II.2 Operational system name

DUACS

II.3 ABC of the altimeter measurement

The Altimetry gives access to the Sea Surface Height (SSH) above the reference ellipsoid(see Figure 1)

$$SSH = Orbit - Altimetric\ Range$$

The Mean Sea Surface (MSS_N) is the temporal mean of the SSH over a period N. It is a mean surface above the ellipsoid of reference and it includes the Geoid.

$$MSS_N = \langle SSH \rangle_N$$

Note that the MSS used in DUACS products (see Table 9 for NRT products; and Table 10 for DT products)is not distributed by CMEMS but is available via the Aviso+ website (with registration) http://www.aviso.altimetry.fr/en/data/products/auxiliary-products/mss.html

The Sea Level Anomaly (SLA_N) is the anomaly of the signal around the mean component. It is deduced from the SSH and MSS_N :

$$SLA_N = SSH - MSS_N$$

The Mean Dynamic Topography (MDT_N) is the temporal mean of the SSH above the Geoid over a period N.

$$MDT_N = MSS_N - Geoid$$

Note that the MDT used in DUACS products (see Table 9 for NRT products; and Table 10 for DT products) is not distributed by CMEMS but is available via the Aviso+ website (with registration) http://www.aviso.altimetry.fr/en/data/products/auxiliary-products/mdt.html

The Absolute Dynamic Topography (ADT) is the instantaneous height above the Geoid. The geoid is a gravity equipotential surface that would correspond with the ocean surface if ocean was at rest (i.e. with no currents under only the gravity field). Then, when the ocean is also influenced by wind, differential heating and precipitation and other sources of energy, the ocean surface moves from the geoid. Thus, the departure from the geoid provides information on the ocean dynamics.

The ADT is the sum of the SLA_N and MDT_N:

$$ADT = SLA_N + MDT_N = SSH - MSS_N + MDT_N$$

The reference period N considered can be changed as described in Pujol et al (2016).

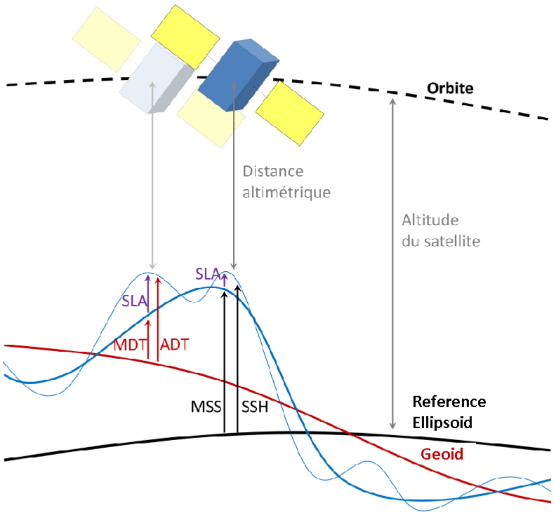

- **SSH: Sea Surface Height**
- **SLA: Sea Level Anomaly**
- **MSS: Mean Sea Surface**
- **ADT: Absolute Dynamic topography**
- **MDT: Mean Dynamic Topography**

Figure 1: Different notions of sea surface height used in altimetry

II.4 Production centre description for the version covered by this document

II.4.1 Introduction

DUACS system is made of two components: a Near Real Time one (NRT) and a Delayed-Time (DT also named REP) one.

In NRT, the system's primary objective is to provide operational applications with directly usable high quality altimeter data from all missions available.

In DT, it is to maintain a consistent and user-friendly altimeter database using the state-of-the-art recommendations from the altimetry community.

The following figure gives an overview of the system, where processing sequences can be divided into 7 main steps:

- acquisition
- Pre-processing homogenization
- Input data quality control
- multi-mission cross-calibration
- along-track products generation
- merged products generation
- final quality control

The processing is similar for NRT and DT component. We give here a description of the different steps of the processing. The reader can also see Pujol et al (2016) for complementary details.

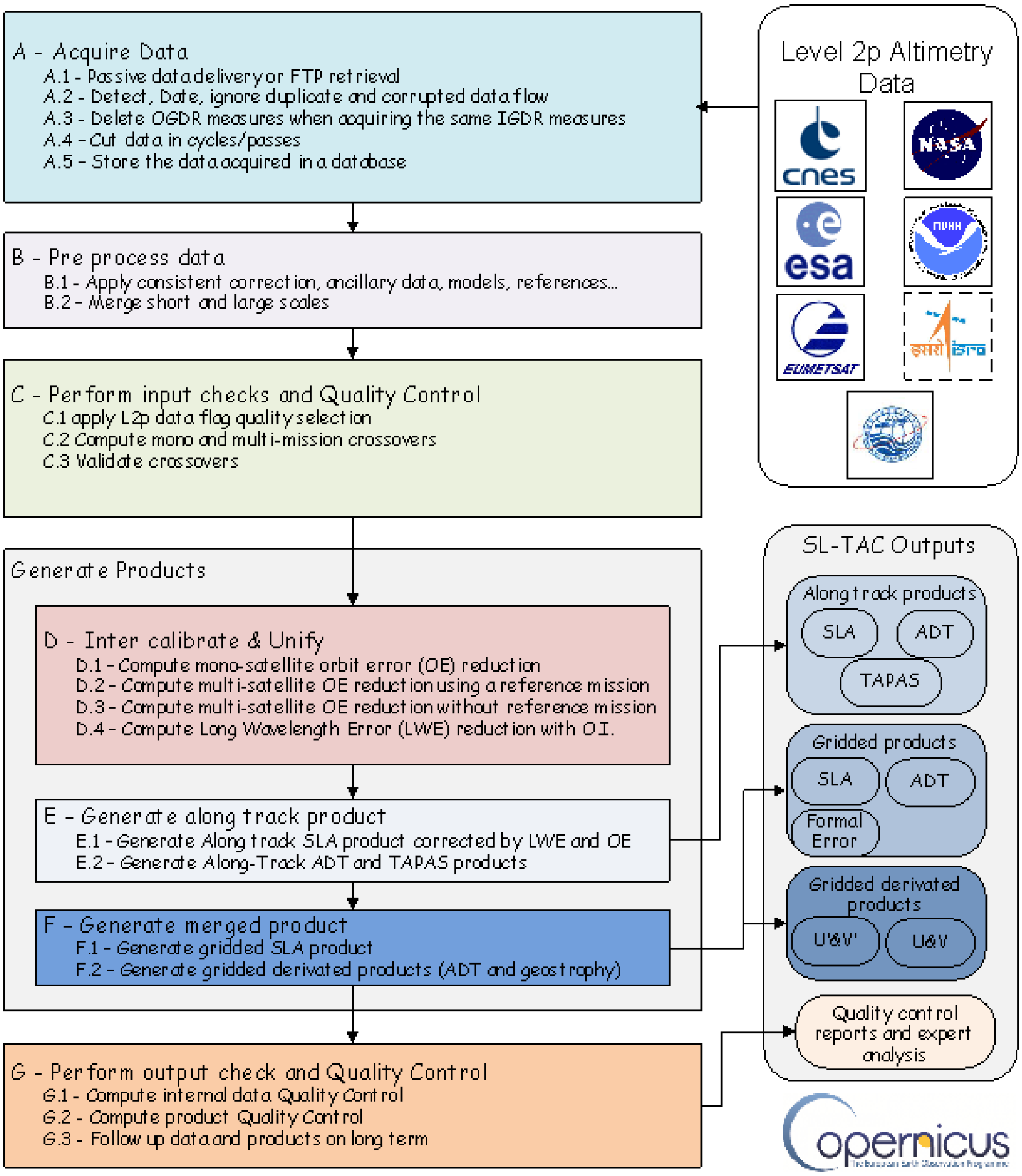

Figure 2: DUACS system processing

II.4.2 Altimeter Input data description

The altimeter measurements used in input of the DUACS system consist in Level2p products from different missions, that are available under three forms, with different delay of availability:

- Fast delivery or Near Real Time products (OGDR or NRT). These products do not always benefit from precise orbit determination, nor from some external model-based corrections (Dynamic Atmospheric Correction (DAC), Global Ionospheric Maps (GIM)).
- The Intermediate or Slow Time Critical products (IGDR or STC) that are the latest high-quality altimeter data produced in near-real-time

- Delayed Time or Non Time Critical product (GDR or NTC).

Details of the different L2p altimeter products sources and delay of availability are given in Table 7.

OGDR/NRT and IGDR/STC are both used in operational system while GDR/STC are involved in delayed time processing.

Altimeter mission	Type of product	Source	Availability delay
Sentinel-3A	NRT	ESA/EUMETSAT	~3h
	STC		~48h
	NTC		~1 month
Jason-3	OGDR	EUMETSAT/NOAA	~3 to 5h
	IGDR	CNES	~24h
	GDR	CNES	~1 to 2 months
Jason-2	OGDR	EUMETSAT/NOAA	~3 to 5h
	IGDR	CNES	~24h
	GDR	CNES	~1 to 2 months
Cryosat-2	OGDR	ESA/CNES	Best effort
	IGDR		~48h
	GDR	ESA	Best effort
Saral/AltiKa	OGDR	ISRO/EUMETSAT	~3 to 5h
	IGDR	CNES	~48h
	GDR	CNES	~2 months
HY-2A	GDR	NSOAS	Best effort
Topex/Poseidon	GDR	CNES	Reprocessing only
Jason-1	GDR	CNES	Reprocessing only
Envisat	GDR	ESA	Reprocessing only
ERS-1	GDR	ESA	Reprocessing only
ERS-2	GDR	ESA	Reprocessing only
Geosat Follow On	GDR	NOAA	Reprocessing only

Table 7: Source and delay of availability of the different altimeter data used in input of DUACS system

Altimeter mission	Cycle duration (days)	Latitude range (°N)	Number of track in the cycle	Inter-track distance at equator (km)	Sun-synchronous	Dual-frequency Altimeter	Radiometer on board	input data availability Start-End dates
Sentinel-3A	27	±81.5	770	~100	Yes	Yes	Yes	2016/12/13 (cycle 12) Ongoing
Jason-3	10	±66	254	~315	No	Yes	Yes	2016/02/17 (cycle 1) Ongoing
Jason-2	10	±66	254	~315	No	Yes	Yes	2008/07/12 (cycle1) 2016/10/02 (cycle 303)
Jason-2 Interleaved	10	±66	254	~315				2016/10/13 (cycle 305) Ongoing
Cryosat-2	29 (sub cycle)	±88	840	~98	No	No	No	2011/01/01 (cycle 13) Ongoing
Saral/AltiKa	35	±81.5	1002	~80	Yes	No	Yes	2013/03/14 (cycle 1) 2016/07/04 (cycle 35)

SARAL-DP/AltiKa	?	±81.5	?	-				2016/07/04 (cycle 100) Ongoing
HaiYang-2A	14	±81	386	~210	Yes	Yes	Yes	2011/10/01 (cycle 1) 2016/05/03 (cycle 120)
HaiYang-2A geodetic	168	±81	-	-				2016/03/24 (cycle 1) Ongoing
Topex/Poseidon	10	±66	254	~315	No	Yes	Yes	1992/09/25 (cycle 1) 2002/08/21 (cycle 365)
Topex/Poseidon Interleaved	10	±66	254	~315				23/08/2002 (cycle 366) 2005/10/08 (cycle 481)
Jason-1	10	±66	254	~315	No	Yes	Yes	2002/01/15 (cycle 1) 2009/01/26 (cycle 259)
Jason-1 Interleaved	10	±66	254	~315				2009/02/10 (cycle 262) 2012/03/03 (cycle 374)
Jason-1 Geodetic	10.91	±66	280	-				2012/05/07 (cycle 500) 2013/06/21 (cycle 537)
Envisat	35	±81.5	1002	~80	Yes	Yes (S-band lost after cycle 65)	Yes	2002/04/10 (cycle 5) 2010/10/18 (cycle 93)
Envisat-New	30	±81.5	862	-				2010/11/27 (cycle 96) 2012/04/08 (cycle 113)
ERS-1	35	±81.5	1002	~80	Yes	Yes	Yes	1992/10/23 (cycle 15) 1993/12/20 (cycle 27) And 1995/03/240 (cycle 41) 1996/06/02 (cycle 53)
ERS-1 geodetic	168	±81.5	-	-				04/10/1994 (cycle 30) 03/21/1995 (cycle 40)
ERS-2	35	±81.5	1002	~80	Yes	Yes	Yes	1995/05/15 (cycle 1) 2011/07/04 (cycle 169)
Geosat Follow On	17	±72	488	~165	No	No	Yes	2000/01/07 (cycle 37) 2008/09/07 (cycle 222)

Table 8: Altimeter missions characteristics and L2p products availability period.

II.4.3 Acquisition processing

The acquisition process is twofold:

- straightforward retrieval and reformatting of altimeter data
- synchronization process.

The measurements ([O/I]GDR or equivalent) from different altimeters are retrieved. DUACS system takes in input L2P altimeter products;

The acquisition software detects, downloads and processes incoming data as soon as they are available on remote sites (external database, FTP site). Data are split into passes if necessary. This processing step delivers "raw" data, that is to say data that have been divided into cycles and passes, and ordered chronologically.

In NRT processing, the acquisition step uses two different data flows: the OGDR/NRT flow (within a few hours), and the IGDR/STC flow (within a few days). For each OGDR/NRT input, the system checks that no equivalent IGDR/STC entry is available in the data base before acquisition; for each IGDR/STC input, the system checks and delete the equivalent OGDR/NRT entry in the data base. These operations aim to avoid duplicates in DUACS system. This processing is summarized in Figure 3.

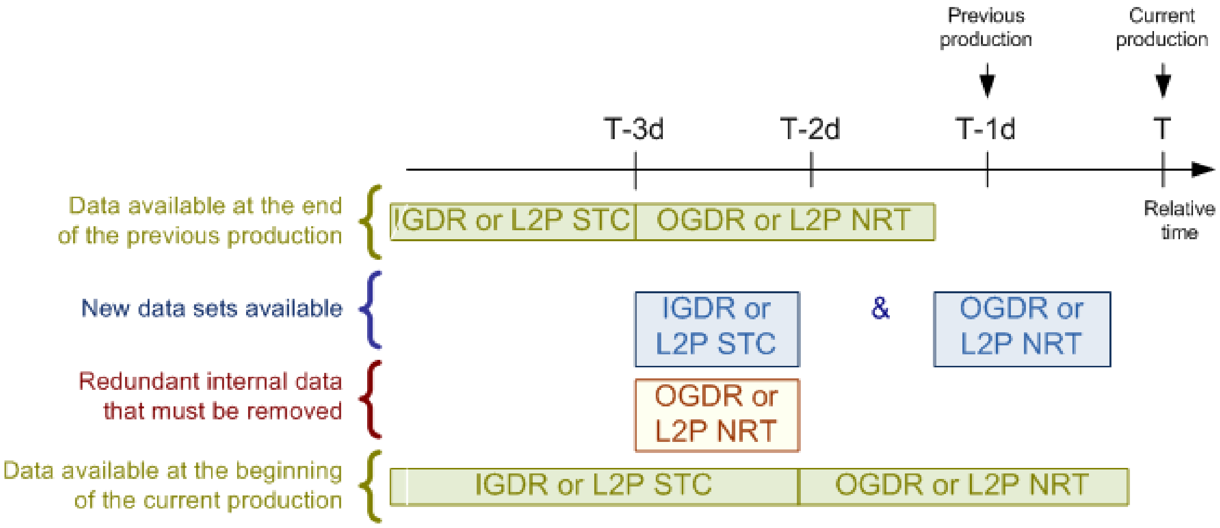

Figure 3: Overview of the near real time system data flow management

The number of altimeter processed varies with time as summarized in **Figure 4** and **Figure 5**.

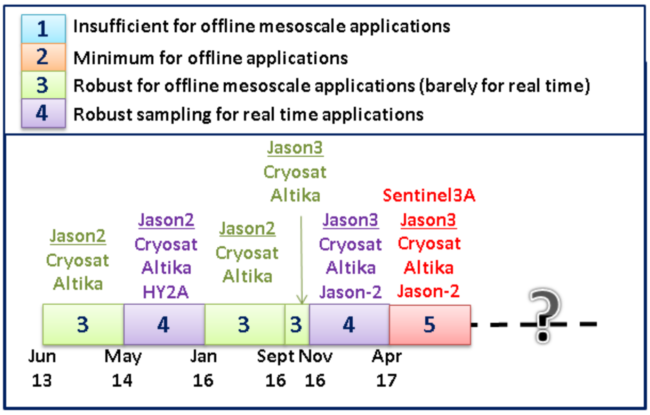

Figure 4: Evolution of the number of altimeters processed in NRT conditions. The reference mission is underlined.

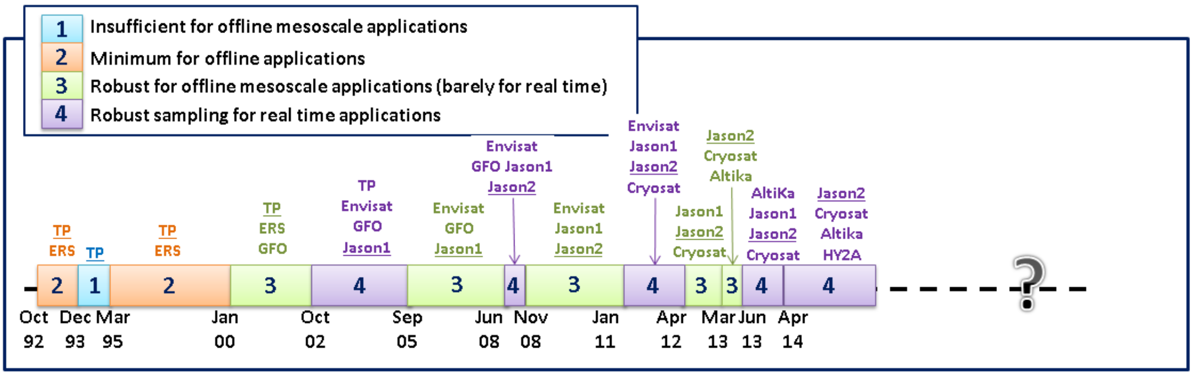

Figure 5: Evolution of the number of altimeters processed in REP conditions. The reference mission is underlined.

II.4.4 Input data quality control

The L2 Input Data Quality Control is a critical process applied to guarantee that DUACS uses only the most accurate altimeter data.DUACS system is supplied with L2p altimeter products that include a quality flag for each measurement. The valid data selection is directly based on this quality flag.Thanks to the high quality of current missions, this process rejects a small percentage of altimeter measurements, but these erroneous data could be the cause of a significant quality loss.

The L2p quality control relies on standard raw data editing with quality flags or parameter thresholds, but also on complex data editing algorithms based on the detection of erroneous artifacts, mono and multi-mission crossover validation, and macroscopic statistics to edit out large data flows that do not meet the system's requirements. Details of threshold editing can be found in the handbook of each altimeter mission [e.g. Aviso/SALP 2016a, 2016b, 2016c] as well as Cal/Val reports [e.g. Aviso/SALP (2015)].

II.4.5 Homogenization and cross-calibration

Homogenization and cross-calibration are done at different steps of the processing.

The first homogenization step consists of acquiring altimeter and ancillary data from the different altimeters that are a priori as homogeneous as possible. The DUACS processing is based on the altimeter standards given by L2p products. They include the most recent standards recommended for altimeter global products by the different agencies and expert groups such as OSTST, ESA Quality Working groups or ESA SL_cci project. Each mission is processed separately as its needs depend on the input data. When available, a specific standard recommended for regional processing can be applied by DUACS. The list of corrections and models currently applied in NRT processing is provided in Table 9. The list of corrections and models currently applied in REP/DT processing is provided in Table 10.

	J3	J2 interleaved	Cryosat-2	SARAL-DP/AltiKa	Sentinel-3A
Product standard ref	GDR-D		CPP (Boy et al, 2017)	T version, Patch 2	L2p products [Aviso+, 2016d]
Orbit	CNES MOE GDR-E				
Ionopheric	dual-frequency altimeter range measurements		GIM model [Iijima et al., 1999]		
Dry troposphere	Model computed from ECMWF Gaussian grids (new S1 and S2 atmospheric tides are applied)				
Wet troposphere	JMR/AMR radiometer		Model computed from ECMWF Gaussian grids	ALTIKA_RAD radiometer	
DAC	MOG2D High Resolution forced with ECMWF pressure and wing fields (S1 and S2 were excluded) + inverse barometer computed from rectangular grids .(Carrere and Lyard, 2003)				
Ocean tide	FES2014 (S1 and S2 are included) [Carrere et al, 2015]				
Pole tide	[Wahr, 1985]				
Solid earth tide	Elastic response to tidal potential [Cartwright and Tayler, 1971], [Cartwright and Edden, 1973]				
Loading tide	GOT4v8 (S1 parameter is included)				
Sea state bias	Non parametric SSB (using J2 cycles 1 to 36 with GDR-D standards) (Tran, 2012)		Non parametric SSB (using J1 GDR-C standards)	Hybrid SSB (Scharroo et al, 2013))	
Mean Profile/ Mean Sea Surface	Computed with 20 years of TP/J1/J2 measurements; referenced to the 1993-2012 period with DT2014 standards (Pujol et al, 2016)		CNES_CLS_2015 referenced to the 1993-2012 period (Schaeffer et al, 2016)		
Mean Dynamic Topography	Global and Europe area: MDT_CNES_CLS13 (Mulet et al, 2013)corrected to be consistent with the 20-year reference period used for the SLA. Mediterranean Sea: SMDT_MED_2014 (Rio et al, 2014b)				

Table 9: Standards of the different corrections applied on altimeter measurements in NRT processing.

	Sentinel-3A	**Jason-3**	**OSTM/ Jason-2**	**Jason-1**	**Topex/ POSEIDON**	**ERS-1**	**ERS-2**	**ENVISAT**	**Cryosat-2**	**SARAL/ AltiKa**
Product standard ref	GDR-E	GDR-D	GDR-D	GDR-D	GDR-C	OPR		GDRV2.1+	GOP ESA	GDR-T patch2
Orbit	Cnes POE (GDR-E)	Cnes POE (GDR-E)	Cnes POE (GDR_D for cycles ≤253 and GDR-E afterward)	Cnes POE (GDR_D)	GSFC (ITRF2005, Grace last standards)	Reaper [Rudenko et al., 2012]		Cnes POE (GDR-D)	Cnes POE (GDR-D for cycle ≤66 and GDR-E afterwards) & since cycle 88: ESA GOP (Geophysical Oecan Products)	Cnes POE (GDR-D for cycle ≤23 and GDR-E afterward)
Ionophere	Iono filtre SLOOP	dual-frequency altimeter range measurements			dual-frequency altimeter range measurements (Topex), Doris (Poseidon)	Reaper (NIC09 model, Scharro and Smith, 2010)	Bent model (cycle ≤ 36), GIM model (cycle > 36) [Iijima et al., 1999]	dual-frequency altimeter range measurement (cycle 6-64) and GIM model >cycle 65 [Iijima et al., 1999] corrected from 8 mm bias	GIM model [Iijima et al., 1999]	
Dry troposphere	Model computed from ECMWF Gaussian grids (new S1 and S2 atmospheric tides are applied)			Model computed from ECMWF rectangular grids (new S1 and S2 atmospheric tides are included)	Model computed from ERA Interim Gaussian grids (new S1 and S2 atmospheric tides are applied)			Model computed from ECMWF Gaussian grids (new S1 and S2 atmospheric tides included)	Model computed from ECMWF Gaussian grids (new S1 and S2 atmospheric tides included)	Model computed from ECMWF Gaussian grids (new S1 and S2 atmospheric tides included)
Wet troposphere	From S3A-AMR radiometer	J3 radiometer	JMR radio meter	AMR radiometer (enhancement product)	TMR radiometer [Scharoo et al. 2004]	MWR radio meter	MWR corrected for 23.6Ghz TB drift [Scharoo et al. 2004] before Neutral Network algorithm	MWR ≥50km from the coast + ECMWF between 10-50 km from the coast (cycle ≤94); MRW (cycle >94)	ECMWF model	WMR radiometer
DAC	MOG2D High Resolution forced with ECMWF pressure and wing fields (S1 and S2 were excluded) + inverse barometer computed from rectangular grids .				MOG2D High Resolution forced with ERA Interim pressure and wing fields (S1 and S2 were excluded) + inverse barometer computed from rectangular grids .			MOG2D High Resolution forced with ECMWF pressure and wing fields (S1 and S2 were excluded) + inverse barometer computed from rectangular grids .		
Ocean tide	FES2014	GOT4v8 (S1 and S2 are included)								
Pole tide	[DESAI, 2015]	[Wahr, 1985]								
Solid earth tide	Elastic response to tidal potential [Cartwright and Tayler, 1971], [Cartwright and Edden, 1973]									
Loading tide	FES2014	GOT4v8 (S1 parameter is included)								

Sea state bias	Non parametric SSB [N. Tran]	Non parametric SSB [Tran, 2012] (using J2 cycles 1 to 36 with GDR-D standards)	Non parametric SSB [Tran, 2012] (using J1 cycles 1 to 111 with GDR-C standards and GDR-D orbit)	Non parametric SSB [N. Tran and al. 2010] (using cycles 21 to 131 with GSFC orbit for TP-A; cycles 240 to 350 with GSFC orbit for TP-B)	BM3	Non parametric SSB (using cycles 70 to 80 with DELFT orbit and equivalent of GDR-B standards)	Non parametric SSB [Tran, 2012] compatible with enhanced MWR	Non parametric SSB from J1, with unbiased sigma0	Hybrid SSB from R. Scharroo et al (2005)
Mean Sea Surface	CNES-CLS-2015	CNES_CLS_2011 referenced to the 1993-2012 period							

Table 10: Standards of the different corrections applied on altimeter measurements in DT processing.

Input L2p products includes a first cross-calibration processing that consists of ensuring mean sea level continuity between the three altimeter reference missions. This step, crucial for climate signals, is done as accurately as possible in REP/DT conditions, taking into account both the global and regional biases, as presented in Pujol et al (2016). In NRT conditions, the accuracy of this cross-calibration step is reduced due to the temporal variability of the orbits solutions. Only the global bias between the reference mission is usually corrected.

Nevertheless, they are not always coherent at large regional scales due to various sources of geographically correlated errors (instrumental, processing, orbit residuals errors). Consequently, the DUACS multi-mission cross-calibration algorithm aims to reduce these errors in order to generate a global, consistent and accurate dataset for all altimeter constellations. This step processing consists of applying the Orbit Error Reduction (OER) algorithm. This process consists of reducing orbit errors through a global minimization of the crossover differences observed for the reference mission, and between the reference and other missions also identified as complementary and opportunity missions, as presented by Le Traon and Ogor (1998). Multi-satellite crossover determination is performed on a daily basis. All altimeter fields (measurement, corrections and other fields such as bathymetry, MSS,...) are interpolated at crossover locations and dates. Crossovers are then appended to the existing crossover database as more altimeter data become available. This crossover data set is the input of the OER method. Using the precision of the reference mission orbit (Topex/Jason series), an accurate orbit error can be estimated. This processing step is applied on GDR/NTC as well as on IGDR/STC measurements. It does not concern OGDR/NRT.Specifically, to the OGDR measurements processing, the DUACS system includes SLA filtering. The reduced quality of the orbit solution indeed limits the use of the long-wavelength signal with these OGDR products. The DUACS processing extracts from these data sets the short scales (< ~900km) which are useful to better describe the ocean variability in real time, and merge this information with a fair description of large scale signals provided by the multi-satellite observation in near real time. Finally, a "hybrid" SLA is computed. This OGDR processing is summarized in Figure 6.

The last step consists of applying the long wavelength error (LWE) reduction algorithm based on Optimal Interpolation (see for instance; Le Traon et al, 2003; Pujol et al, 2016). This process reduces geographically-correlated errors between neighboring tracks from different sensors. This optimal-interpolation based empirical correction also contributes to reduction of the residual high frequency signal that is not fully corrected by the different corrections that are applied (mainly the Dynamic Atmospheric Correction and Ocean tides).

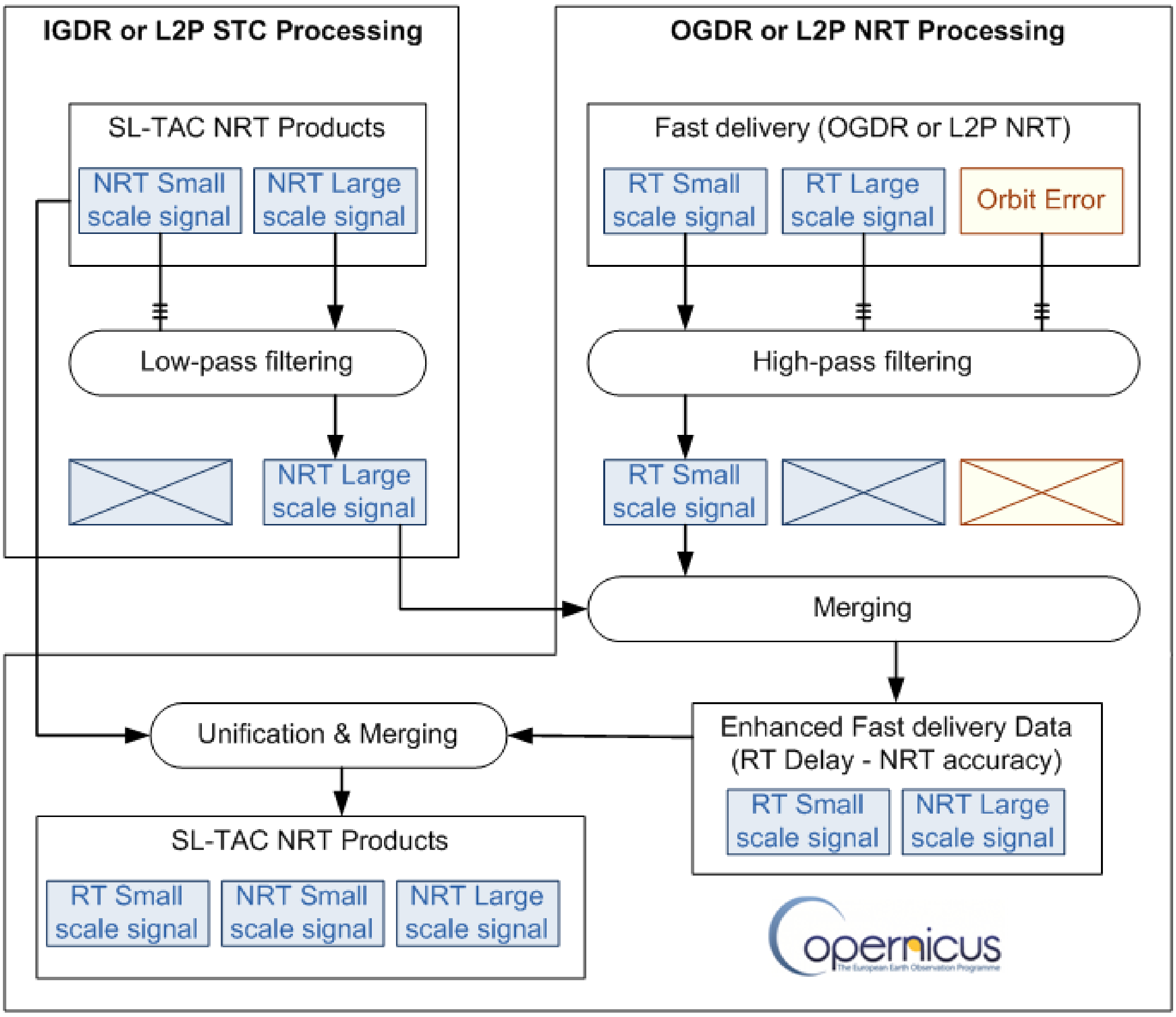

Figure 6: Merging pertinent information from IGDR and OGDR processing

II.4.6 Along-track (L3) products generation

II.4.6.1 SLA computation

The Sea Level Anomalies (SLA) are used in oceanographic studies. They are computed from the difference of the instantaneous SSH minus a temporal reference. This temporal reference can be a Mean Profile (MP) in the case of repeat track or a gridded Mean Sea Surface (MSS) when the repeat track cannot be used. The errors affecting the SLAs, MPs and MSS have different magnitudes and wavelengths. The computation of the SLAs and their associated errors are detailed in Dibarboure et al, 2011 and Pujol et al, 2016. Both MP and MSS are referenced to the same reference period as specified in Table 10. The methodology to change the reference period is presented in Pujol et al 2016.

Altimeter mission,	**MP description**
Topex/Poseidon, Jason-1,	MP computed with Topex/Poseidon [1993, 2003; cycles 11 to

OSTM/Jason-2, Jason-3	343], Jason-1 [2002, 2008; cycles 11 to 250] and Jason-2 [mid 2008, 2013; cycles 1 to 167] measurements. Referenced to the [1993, 2012] period (Pujol et al, 2016)
ERS-1/ERS-2, Envisat,SARAL/AltiKa	MP computed with ERS-2 [1995, 2002; cycles 1 to 85] and Envisat [2002, 2010; cycles 6 to 64] measurements. Referenced to the [1993, 2012] period (Pujol et al, 2016)
Topex/Poseidon interleaved, Jason-1 interleaved;OSTM/Jason-2 interleaved	MP computed with Topex/Poseidon interleaved [2003, 2006; cycles 369 to 479] and Jason-1 interleaved [mid 2012, 2013; cycles 500 to 524] measurements. Referenced to the [1993, 2012] period (Pujol et al, 2016)
Geosat Follow-On	MP computed with Geosat Follow On [2001, 2007; cycles 37 to 187] measurements. Referenced to the [1993, 2012] period (Pujol et al, 2016)
Cryosat-2	No MP available for theses missions. A gridded MSS is used as described in section II.4.5
SARAL-DP/AltiKa	
Sentinel-3A	
Jason-1 geodetic	
Envisat new	

Table 10: MPs and MSS used for the SLA computation along the different altimeters tracks (see Table 9 to see which products are using MP).

II.4.6.2 Along track (L3) noise filtering

The filtering processing consists in removing from along-track measurements the noise signal and short wavelength affected by this noise. This processing consists in a low-pass filtering with a cut-off wavelength of 65km over the global ocean. This cut-off wavelength comes from the study by Dufau et al. (2016) and is discussed in Pujol et al, (2016). It represents the minimum wavelength associated with the dynamical structures that altimetry would statistically be able to observe with a signal-to noise ratio greater than 1. The cut-off is reduced for regional products in order to preserve as much as possible the short wavelength signal. The different cut-off wavelength used are summarized in Table 11.

The filtered along-track products can be subsampled before delivery in order to retain every second point along the tracks, leading to a nearly 14 km distance between successive points. Because some applications need the full resolution data, the non-filtered and non-sub-sampled products are also distributed in REP/DT mode and over some regions in NRT mode. The different subsamplings are summarized in Table 11.

Product considered	Filtering cut-off wavelength (km)	Distance between two points after subsampling (km)
Global*	~65	14
Mediterranean Sea*@	~40	14
Black Sea*	~40	7
Europe@	~35	7
Arctic	~35	14

**Unfiltered and Unsubsampled products are also provided in REP L3 products*

@Unfiltered and Unsubsampled products are provided in "PHY_ASSIM_L3" NRT products

Table 11: Filtering and subsampling parameters used for L3 products

II.4.7 SLA Gridded (L4) products generation

The L4 product generation processing methodology consists in an optimal interpolation processing as fully synthesized in Pujol et al (2016).

In the REP/DT processing, the products can be computed optimally with a centered computation time window of ±6weeks around the date of the map to be computed.

In the NRT processing, contrary to REP/DT case, the products cannot be computed with a centered computation time window: indeed, as the future data are not available yet, the computation time window is not centered. Only data over the period [D-7weeks, D] are used, where D is the date of the production considered. For each day of NRT production, three merged maps are produced dailyand delivered to the users (Figure 7): :

- A 0-day delay (i.e. map centered on day D), which represents a preliminary map production
- A 3-day delay (i.e. map centered on day D-3days), which represents an intermediate map production. When available, this map replaces the 0-day delay map
- A 6-day delay (i.e. map centered on day D-6days), which represents a final NRT map production. When available, this map replaces the 3-day delay map

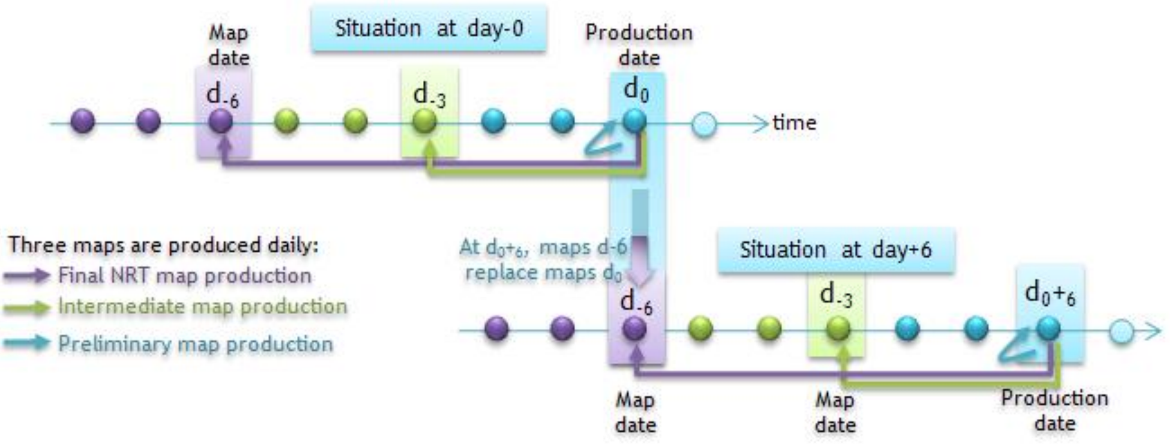

Figure 7: Three merged maps are produced daily: final map (d-6), intermediate map (d-3) and preliminary map (d0)

Both for the REP and NRT, the maps are centered on mid-night.

Note however that the spatial and temporal scales of the variability that is resolved in the DUACS merged products data set are imposed by the temporal correlation function used in the OI mapping procedure, as described in Pujol et al (2016).

II.4.7.1 Number of satellites to compute the maps

Both in REP/DT and NRT processing, the maps are computed with all the satellites available. This allows an improved signal sampling when more than 2 altimeters (corresponding to the minimal constellation) are available. The mesoscale signal is indeed more accurately reconstructed during these periods (Pascual and al, 2006), when omission errors are reduced by the altimeter sampling. The all-sat-merged series is however not homogeneous in time due to the evolutions of the altimeter constellation (see **Table 1**, **Figure 4** and **Figure 5**)

II.4.7.2 Formal mapping error

The formal mapping error represents a purely theoretical mapping error. It mainly represents errors induced by the constellation sampling capability and consistency with the spatial/temporal scales considered, as described in Le Traon et al (1998) or Ducet et al (2000).

II.4.8 L4 Derived product generation

The L4 derived products consist of the Absolute Dynamic Topography (ADT) (maps and along-track) and maps of geostrophic currents (absolute and anomalies).

The ADT products are obtained by adding a Mean Dynamic Topography (MDT) to the SLA field. The MDT used in the DT2014 reprocessing is described in Table 9.

The geostrophic current products disseminated to users are computed using a 9-point stencil width methodology (Arbic et al, 2012) for latitudes outside the ±5°N band. In the equatorial band, the Lagerloef methodology (Lagerloef et al, 1999) introducing the β plane approximation is used.

The reader can refer to Pujol et al (2016) for additional details.

II.4.9 L3 and L4 Quality control

The production of homogeneous products with a high quality data and within a short delay is the key feature of the DUACS processing system. But some events (failure on payload or on instruments, delay, maintenance on servers), can impact the quality of measurements or the data flows. A strict quality control on each processing step is indispensable to appreciate the overall quality of the system and to provide the best user services.

The Quality Control is the final process used by DUACS before product delivery. In addition to daily automated controls and warnings to the operators, each production delivers a large QC Report composed of detailed logs, figures and statistics of each processing step. An overview of the diagnostics used is given in §III. Altimetry experts analyze these reports twice a week (only for internal validation, those reports are not disseminated).

III VALIDATION FRAMEWORK

The validation aims to control the quality of the external products and the performances of the key processing steps. Different points are assessed by the validation task:

- The data availability and spatial/temporal coverage
- the multi-mission homogenization processing
- the ocean signal consistency

The following table lists the different metrics that are used. They mainly consist in an analysis of the SLA field at different steps of the processing; check consistency of the SLA along the tracks of different altimeters and between gridded and along-track products; and comparison of the different variable fields (SLA, ADT, geostrophic current) with external in-situ measurements.

Assessment of the DUACS products are also completed by specific studies, done in coordination with other projects (e.g. ESA SL_cci, CNES SALP) that aim to characterize the errors observed on specific fields, wavelengths and timescales.

Name	**Description**	**Ocean parameter**	**Supporting reference dataset**	**Quantity**
SLA_L2-NC--AVAIL	Number of altimeter measurement available/rejected	Sea Level Anomaly	None	Missing/valid/invalid data are identified over the data flow processed Temporal evolution on the number of measurements on a daily basis and/or along each track of the altimeter considered.
SLA_L2-NC-ALT--MEAN	SLA differences at mono- and multi-missions crossover positions	Sea Level Anomaly	None	Mean difference between two SLA measurements corresponding to altimeter tracks cross-over positions. The statistic is averaged over 7 days The performance of the product before and after OrbitError correction are compared
SLA_L2-NC-ALT-STD				Standard deviation of the difference between two SLA measurements corresponding to altimeter tracks cross-over positions. The statistic is averaged over 7 days The performance of the product before and after OrbitError correction are compared
SLA_L2-NC-ALT-AVAIL				Number of SLA measurements corresponding to altimeter tracks cross-over positions. The statistic is averaged over 7 days The performance of the product before and after OrbitError correction are compared
SLA_LWENC-VAR	Variance of the Long Wavelength Error correction applied on SLA products	LWE correction	None	Variance of the LWE correction averaged over the last 49 days
SLA_LWE--NC-DIFFVAR	Difference of variance of the SLA with and without LWE correction applied	Sea Level Anomaly	None	Difference of the variance of the SLA with and without LWE correction applied. Statistics averaged over the last 49 days.
SLA_SW-NC-VAR	Variance of the short wave SLA signal	Sea Level Anomaly; measurement noise	None	Variance of the short wave signal (<65km) filtered from along-track products Temporal daily statistics evolution. Regional mean statistics computed over the last 49 days.
SLA-D-NC-MEAN-<REGIONS>	SLA signal monitoring	Sea Level Anomaly	None	Mean of the along-track SLA (L3) over different regions averaged on a daily basis
SLA-D-NC-STD-<REGIONS>				Standard deviation of the along-track SLA (L3) over different regions averaged on a daily basis
SLA-D-NC-AVAIL-<REGIONS>				Number of along-track SLA (L3) over different regions averaged on a daily basis

SLA-NC-PSD-<REGIONS>	SLA signal spectral content	Sea Level Anomaly	None	Spectral decomposition of the Sla signal over different regions
SLA-D-NC-ALT-MEANDIFF-<REGIONS>	Difference between two SLA map products	Sea Level Anomaly	None	Mean difference between two SLA map products: Map of days D0 and Day D-7 Map of day D0 merging all the altimeters available and only one altimeter. Map of day D0 computed over global ocean and regional area
SLA-D-NC-MEAN-<REGIONS>	SLA signal monitoring	Sea Level Anomaly	None	Mean of the map SLA (L4) over different regions averaged on a daily basis
SLA-D-NC-STD-<REGIONS>				Standard deviation of the map SLA (L4) over different regions averaged on a daily basis
SLA-D-NC-AVAIL-<REGIONS>				Number of grid node defined by the map SLA (L4) over different regions averaged on a daily basis
SLA-D-NC-MERR-<REGIONS>	Formal Mapping Error (ERR) monitoring	Formal Mapping Error	None	Mean of the ERR associated to the map SLA (L4) over different regions averaged on a daily basis
MKE-D-SURF-NC-MEAN-<REGIONS>-3MONTHLY	EKE monitoring	Eddy Kinetic Energy	None	Mean of the EKE deduced from the map SLA (L4) over different regions averaged on a daily basis Regional mean over the last 3 months
SLA-D-NC-DFS_MEAN	Contribution of the different altimeters to the map product	DFS	None	Mean contribution of the different altimeters available to the merged SLA map product
DHA_2000m-SURF-CLASS4-PROF-MEAN	DHA comparison with in situ Temperature/Salinity profiles estimation	Dynamic Height Anomalies	ARGO Temperature/Salinity profiles	Monitoring of the differences between Altimetry and T/S DHA estimation, at global and regional scales.
SLA-D-CLASS2-TG-RMSD	SLA comparison with in situ Tide Gauges measurements	SLA	Tide Gauges measurements (PSMSL & GLOSS CLIVAR)	Map of the variability of the differences between altimetry and TG measurements
SLA-D-CLASS4-ALT--RMSD	SLA comparison with independent altimeter along-track measurements	SLA	Altimeter measurements non used in map products construction	Map of the variability of the differences between altimetry and independent along-track measurements
UV-SURF-D-CLASS4--BUOY-RMSD	U&V geostrophic current comparison with in situ drifters measurements	geostrophic current	Drifters measurements (AOML)	Map of the variability of the differences between altimetry and drifters measurements

Table 12: List of the metrics used for DUACS products operational validation

IV VALIDATION RESULTS

IV.1 Variable SLA

IV.1.1 Level-3 along-track

IV.1.1.1 The main sources of errors

The along-track SLA product is affected by different errors :

- Instrumental errors: they are characteristics of the precision of the instruments and accuracy of the altimeter pointing. They are also representative of the quality of the retracking processing.

  Different corrections are included in the data processing in order to minimize as much as possible these errors. They consist in

  - Mispointing correction: it allows to take into account possible mispointing of the altimeter measurement with respect to the nadir direction
  - Doppler effect correction that takes into account the motion of the satellite
  - The tracking bias that allows to take into account the imprecision of the different algorithms
  - The correction of the Ultra Stable Oscillator (USO) that correct the drift of the instrument
  - The internal calibration that takes into account the transit time of the data in the antenna.

  In spite of these different corrections, part of the instrumental errors remains in the along-track product. They are mainly characterized by uncorrelated measurement noises, discussed in §IV.1.1.2.1.

- Environmental and sea state errors: the path of the electromagnetic signal go through the atmosphere that influences the measurement. In the same way, the sea state bias (presence and shape of the waves and roughness at the surface) also introduce an error on the measurement.

  Different corrections are used in the data processing in order to correct the measurement from atmospheric and sea surface effects:

  - The dry and wet troposphere corrections that correct the path delay effects linked to the presence of dry gases and water vapor in the atmosphere.
  - The ionospheric correction that allows to take into account the effect of the ions present in the atmosphere.
  - The sea state bias correction that correct the effects of the sea surface state on the reflection of the altimeter signal on the surface.

  In spite of these different corrections, part of the environmental errors can still be observed in the along-track SLA signal. They can be spatially and temporally correlated.

- Geophysical errors: They mainly consist in subtracting from the measurement some physical signal that cannot be accurately sampled with the altimeter (due for instance to the inconsistency between the temporal sampling of the altimeter and the temporal scales characteristic of the signal considered) or that are not of interest for the study of the dynamical signal. In that way, different geophysical corrections are applied of the altimeter measurement (geoid, ocean tide, inverse barometer and high frequency wind and pressure effects, etc.). See Table 9 for the details of these corrections.

  The quality of the different corrections, that depends on numerical models, can lead to uncertainty in the different geophysical corrections applied. They are considered as errors on the SLA product, for the main part correlated in space and time.

IV.1.1.2 REP products errors description

IV.1.1.2.1 Uncorrelated errors or noise measurements and mesoscale observability:

The noise measurements are mainly induced by instrumental (altimeter) measurement errors. They are quantified by an analysis of the wavenumber spectra of the SLA (Figure 8). Indeed, the uncorrelated measurement errors is the noise level estimated as the mean value of energy at high wavenumbers (wavelengths smaller than ~5km). It follows the instrumental white-noise linked to the Surface Wave Height. **For the conventional radar altimeter measurement, the inhomogeneity of the sea state within the altimeter footprint also induces an error visible as a "hump" in the wavenumber spectra of the SLA**. It is also included in the noise measurement for the 1Hz product resolution. The full understanding of this hump of spectral energy [Dibarboure et al, 2014] remains to be achieved. This issue is strongly linked with the development of new retracking, new editing strategy or new technology. For the SAR measurement, part of the high frequency signal is characterized by a correlated signal (Figure 8). This signal still need to be fully explained. At this time, it is considered as an additional unknown signal that is assumed to be a "red noise" error considering the ocean geostrophic signal.

The mean 1Hz noise measurement observed for the different altimeters is summarized in Table 2. The products SEALEVEL_GLO_NOISE_L4_NRT_OBSERVATIONS_008_032 and SEALEVEL_GLO_NOISE_L4_REP_OBSERVATIONS_008_033 (Figure 9; example for Jason-2 measurements) give the **spatial variation of this noise, mainly correlated with high/low wave heights areas**. Note that these products give an annual mean status of the noise level. They do not take into account the temporal variability of the wave height that modulate the noise as discussed in Dufau et al (2016).

The presence of noise measurement on along-track products limits the observability of the shorter mesoscales. The SLA power spectrum density analysis was used in order to determine the wavelength where signal and error are on the same order of magnitude (Figure 8). It represents **the minimum wavelength associated with the dynamical structures** that altimetry would statistically be able to observe with a signal-to-noise ratio greater than 1. This wavelength has been found to be variable in space and time (Dufau et al., 2016). The mean value **was found to be nearly 65 km**. It was defined with a single year of Jason-2 measurements, over the global ocean, excluding latitudes between 20°S and 20°N (due, in part, to the limit of the underlying surface quasi-geostrophic turbulence in these areas).

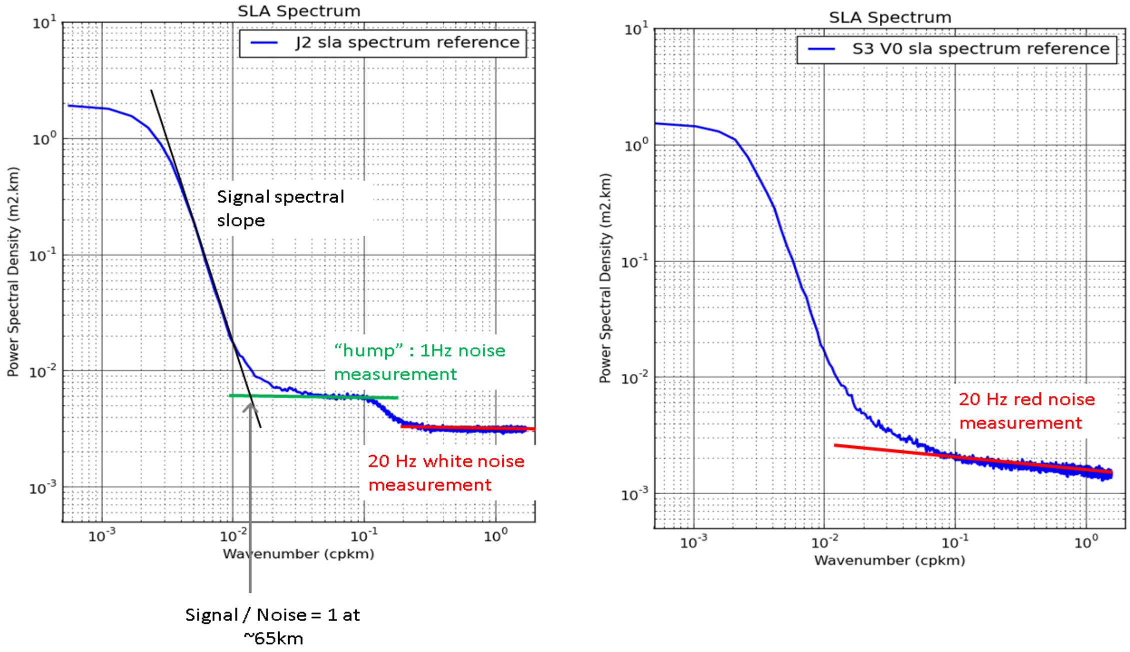

Figure 8 : Mean wavenumber Spectra of Jason-2 (left) and Sentinel-3A (right) SLA over the global ocean

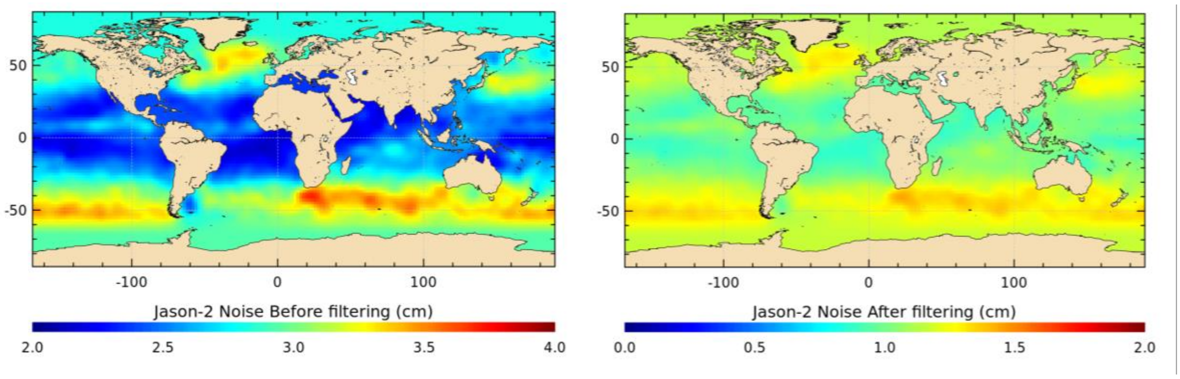

Figure 9: 1Hz noise measurement observed along Jason-2 tracks before (left) and after (right) along-track filtering processing. Note the different colorbars.

IV.1.1.2.2 Errors at climatic scales

In the framework of the ESA SL-cci project, the altimeter measurement errors at climatic scales have been estimated using the Topex/Poseidon; Jason-1; Jason-2 missions. Details on the error budget estimation at climatic scale can be found in Ablain et al (2015). Results are summarized inTable 3.

All the parameters/algorithms involved in the altimeter measurement processing can induce errors at climatic scales. However, some parameters contribute more strongly than others. Thelargest sourcesoferrorsfor Global Mean Sea Level trend estimationhavebeenidentified. They concern the radiometer wet tropospheric correction with a drift uncertainty in the range of 0.2~0.3 mm/yr (Legeais et al., 2014), the orbit error (Couhert et al., 2014) and the altimeter parameters (range, sigma-0, SWH) instabilities (Ablain et al., 2012) with additional uncertainty of the order of 0.1 mm/yr over the whole altimeter period, and slightly more over the first decade (1993-2002) (Ablain et al., 2013). Errors of multi-mission calibration (see §II.4.5) also contribute to the GMSL trend error of about 0.15 mm/yr over the 1993-2010 period (Zawadzki et al., 2015). All sources of errors described above also have had an impact at the inter annual time scale (< 5 years) close to 2 mm over a 2 to 5 years period.

At the regional scale, the regional trend uncertainty ranges from 2 to 3 mm/yr. The Orbit solution remains the main source of the error (in the range of 1~2 mm/yr; Couhert et al., 2014) with large spatial patterns at hemispheric scale. Furthermore, errors are higher during the first decade (1993-2002) where the Earth gravity field models are less accurate. Additional errors are still observed, e.g., for the radiometer-based wet tropospheric correction in tropical areas, other atmospheric corrections in high latitudes, and high frequency corrections in coastal areas. The combined errors give rise to an uncertainty of 0.5~1.5 mm/yr.

IV.1.1.3 NRT vs REP products

The NRT along track L3 products are usually less accurate than the DT ones. The main sources of differences come from the different quality of the L2p altimeter products used in input:

- The Orbit estimation is usually more precise in delayed time conditions due to more precise environmental model (pole position, solar activity) and different techniques (DORIS; GPS) used in real time or delayed time conditions. These differences can induce several cm differences on the Sea level.
- The quality of the Dynamic Atmospheric Correction is improved in DT thanks to a better centering of the filtering windows. For some period the input atmospheric model can also be improved (ERA Interim reanalyzed fields)
- The measurement calibrations(radiometer, altimeter, …)processing are usually more accurate in DT conditions. It is the case for example for the radiometer measurement that can be impacted by drift or significant jump induced by inaccurate NRT calibration processing. Additionally, possible altimeter standard changes in the altimeter L2p products used in input of the DUACS processing can induce jump in the SLA field. The management of these jumps, necessary to ensure a seamless transition for the users, is more precise in DT processing.

Additionally, part of the DUACS processing is also less performant in NRT conditions.

- The multi-mission cross-calibration processing (e.g. Orbit Error Reduction (EOR) and Long Wavelengths Error (LWE); see §II.4.5)is more accurate when using a centered temporal window. This is not possible in NRT processing since measurements in the future are not available.

For these reasons, we do not recommend to use NRT products for climatic scale signal studies (e.g. MSL trend).

IV.1.2 Level-4 gridded

IV.1.2.1 The main sources of errors

The quality of the merged L4 products directly depends on the quality of the L3 products used in input of the L4 processing. Nevertheless, the main source of error comes from the sampling capability of the altimeter constellation. The more altimeters are available, the best is the mesoscale sampling as discussed in §II.4.7. Another source of error for L4 products is directly linked to the methodologies and parameters applied for SLA interpolation on a regular grid. Optimal Interpolation (see §II.4.7) used in DUACS processing does not allow the restitution of the full dynamical spectrum limiting the capability of retrieving small mesoscale in L4 products (Chelton et al, 2011 and 2014).

IV.1.2.2 REP products errors description

The quality of the gridded SLA products was estimated by comparison with independent altimeter along-track and tide gauge measurements, with focus on mesoscale signal. The methodology used and results obtained are fully discussed in Pujol et al (2016). We summarize here the main outcome.

The SLA gridded product errors for the mesoscale signal (Table 4) in the open ocean is estimated to be between 1.4 cm² in low variability areas, and up to 32.5cm² in high variability areas where the altimeter sampling does not allow a full observation of the SLA variability. Compared to the previous version of the products, this error is reduced by a factor of up to 9.9% in high variability areas. The SLA gridded product errors in the coastal areas (< 200 km) are estimated at 8.9 cm², with higher values in high variability coastal areas. This error is globally reduced by 4.1% compared to the previous version of the products. Consistency with TG measurements is improved, especially in different areas such as the northern coast of the Gulf of Mexico, along the Indian eastern coasts and along the US coasts. In this case the reduction of variance of the differences between altimetry and TGs ranges between 2 and up to 10 % of the TG signal, when compared to the results obtained with DT2010 products. In some other coastal areas, degradation is however observed. This is the case in the north Australian and Indonesian areas where it reaches less than 4% of the TG signal.

It is important to note that these results are representative of the quality of the gridded products when only two altimeters are available (see §II.4.3 for the evolution of the altimeter constellation). These can be considered to be degraded products for mesoscale mapping since they use minimal altimeter sampling. On the other hand, the gridded products, during the periods when three or four altimeters were available, benefit from improved surface sampling. The errors during these periods should thus be lower than those estimated here before.

The errors observed on mesoscales also highlight the L4 product spatial resolution capability. As discussed in Pujol et al (2016), SLA gridded product effective resolution is constrained by the altimeter sampling capability and mapping methodology used. The resulting mean spatial resolution of the DT2014 global gridded SLA slightly less than 200 km at mid-latitudes (Chelton et al., 2011, 2014). The comparison with the spectral content computed from full-resolution Saral/AltiKa 1 Hz along-track measurements (not shown) shows that nearly 60% of the energy observed in along-track measurements at wavelengths ranging from 200 to 65 km is missing in the SLA gridded products.

IV.1.2.3 NRT vs REP products

The NRT gridded L4 product are usually less accurate than the DT one. Different factors explain this degradation:

- The reduced accuracy of the different parameter and corrections applied for SLA computation as discussed in §IV.1.1.3
- The availability of altimeter measurements, potentially reduced in NRT condition due to problem on platforms or ground segment, usually retrieved in DT conditions.
- The uncentered temporal window used in NRT L4 processing since measurements in the future are not available, reducing the amount of data by a factor 2 compared to the DT conditions.

The last one is considered as the main sources of errors for mesoscale signal reconstruction in L4 NRT products as discussed in Pascual et al (2008). The authors showed that at least 4 altimeters are required in NRT conditions to retrieved the same accuracy of the DT products generated with only 2 altimeters.

IV.2 Variable ADT

The quality of the ADT field is directly depending on the quality of the SLA and MDT fields (see §II.3). SLA error budget is described in the previous chapter. We focus here on the error budget estimation of the MDT fields.

The MDT standards used for ADT variable construction is described in Table 9. The MDT computation methodology is described in Rio et al (2014a and 2014b). It merges information from a first guess MDT solution, deduced from MSS and Geoid field (case of the global MDT solution) or from numerical ocean models (case of the regional Mediterranean MDT solution), and in-situ measurements (hydrographic profiles and velocity drifters).

The MDT raw validation is based on the comparison with different MDT solutions (e.g. MDT directly deduced from numerical model output) form the mean dynamic height validation. Refined error estimation are obtained using in situ measurements for assessment of the mean geostrophic current. Full validation results of the MDT used for DUACS product generation are presented in Mulet et al (2013) and Rio et al (2014b). We summarize here the main results obtained.

Global Ocean:

The comparison of the Global MDT used in DUACS and equivalent deduced from GLORYS reanalysis underlines significant MDT height differences (> 10 cm) in high variability areas, along the coast and in high latitudes areas. The mean standards deviation of the differences is 4.4 cm.

Mean geostrophic current assessment is done by comparison with independent drifter measurements specifically processed in order to correct for the Ekman currents, the potential wind slippage, the residual ageostrophic currents, and the time dependent geostrophic anomaly (Rio et al., 2014a). Note that in this case, the comparison with drifters is an overestimate of the MDT error since errors of the processed velocities from drifters are also included. Results are presented in Table 13. They show that the difference from drifters ranges between nearly 42 and 47% for the MDT_CNES_CLS13 used in DUACS processing. Results obtain with a MDT solution derived from GLORYS model are slightly degraded.

	MDT CNES-CLS13	**MDT GLORYS2V1**
RMS U	42.17	44.95
RMS V	46.48	51.49

Table 13: RMS differences (expressed in % of drifter velocity variance) between the mean velocities from the different global MDT solutions and independent synthetic mean velocities computed using the real-time SVP velocity dataset distributed by the Coriolis datacenter.

Mediterranean Sea (Rio et al, 2014b):

For the Mediterranean Sea regional MSS, comparison of different solutions underlines differences lower than 2-3 cm. Dynamical geostrophic current estimated using this MDT solution were compared with measurements from independent drifters. The results obtained underscore a good agreement and a significant reduction of the differences compared with the previous regional MDT solution (see Table 14).

	SMDT07	**SMDT-MED-2014**
$V_{Drifte}r-V_{Altimetry}$	15.95	15.0
$V_{Drifte}r-V_{Altimetry}$	14.94	14.1

Table 14: Rms differences (in cm s−1) of altimeter velocities obtained using the old and the new MDT solutions to independent geostrophic velocities. The rms of the zonal (meridian) drifter velocities is 15.5 (15.2) cm s−1. (Rio et al, 2014b)

IV.3 Variable UV (Level-4 gridded)

IV.3.1 REP/DT products error description

The absolute surface currents in the product are calculated by geostrophy from gridded SLA/ADT products (see §II.4.8). The quality of these products strongly depends on the quality of the SLA/ADT field and on the methodology used to estimate the derivate. The comparison with drifter measurements gives an indication of the errors on geostrophic current products. The methodology used for this comparison is described in Pujol et al (2016).

The distribution of the speed of the current (not shown), shows a global underestimation of the current in the altimeter products compared to the drifter observations, especially for currents with medium and strong intensities (> 0.2 m/s). The Figure 10 shows the zonal and meridional differences in 5°x5° boxes between AOML drifters and absolute geostrophic current products over the period [1993, 2012]. The equatorial band was excluded from the analysis due to the geostrophy approximation that do not lead to an accurate estimation of the currents in this region. Elsewhere, the RMS of the differences is around 9.6 (9.6) cm/s for zonal (meridional) component. Locally, the RMS of the differences is higher. It reaches more than 15 cm/s over high variability areas.

The differences with the previous version (DT2010 standards, accessible before April 2014) of the products are discussed in Pujol et al. (2016). They underline that locally the reduction of the errors can reach nearly 10% of the variance of the drifter measurements. However, local degradation is also observed with the new version of the DUACS REP product. It ranges from 2 to 15% of the drifter variance and is mainly located in the tropics. These areas correspond quite well with regions with high amplitudes of the M2 internal tide that are still present in the altimeter measurements and affect the non-tidal signal at wavelengths near 140 km (Dufau et al, 2016; Ray et al, 2015).

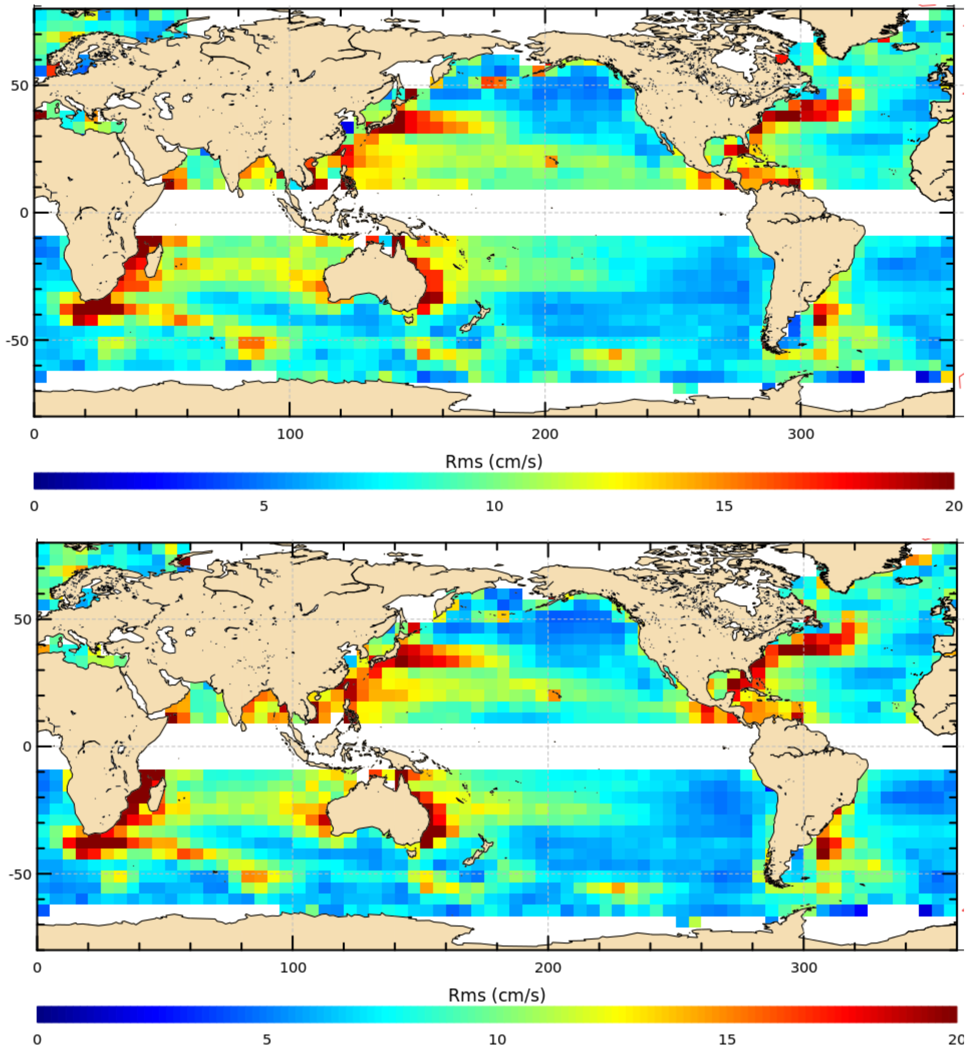

Figure 10: Zonal (top) and meridional (bottom) RMS of the difference between DUACS geostrophic current and drifters measurements over the period [1993-2012] (units: cm/s).

IV.3.2 NRT vs REP/DT products

As discussed in §IV.1.2.3, the quality of the NRT products is reduced in NRT conditions. The quality of the SLA and derived geostrophic current computed in NRT condition is more sensitive to the constellation changes compared to the DT conditions. In that way, changing from 2 to 4 altimeters constellation contributes to reduce the rms of the difference between altimeter NRT product and drifter current measurement by 13% (zonal component) to 19% (meridional component) in area of high variability (equatorial band excluded) (Pascual et al, 2008).

V SYSTEM'S NOTICEABLE EVENTS, OUTAGES OR CHANGES

V.1 NRT sub-system version changes

System version	**Date of the change**	**Description of the change**	**Impact the products quality?**
V15.5	30/11/2015	Delivery of gridded Level4 products	Availability of new products
V15.8	13/04/2016	Improved products: – Use of FES2014 ocean tide correction – Use of MSS DTU13 (Arctic product)	Yes
V16.0	13/09/2016	Integration Jason-3. Introduction of the "sla_assim" product for the "Europe" region	Yes
V16.1	22/11/2016	Integration OSTM/Jason-2 interleaved Change MSS solution for geodetic/drifting missions	Yes
V17.0	19/04/2017	Add new physical variables (adt, uv, ..); product format change	Availability of new variables
		Integration of Sentinel-3A mission. Improved products: – Used new MSS for Arctic regional processing	Yes

V.2 Main constellation events impacting the NRT data availability

Different events can lead to a reduction of the data availability. Such events are usually:

- A change in the altimeter constellation: the loss or introduction of an altimeter in the constellation directly impacts the number of altimeter measurements available.
- For a specific platform, a reduction of the number of altimeter measurements available in input of the DUACS system processing. This can be linked with an anomaly onboard the platform or on the ground segment, preventing the data reception and impacting the L0 to L2 processing. It can also be induced by an abnormal acquisition by the DUACS system.
- An increase of invalid measurements in input of the DUACS system processing. This is usually linked with specific platform events (e.g. maneuvers), but can also be induced by L0-L2 processing anomalies or specificities. In some rare cases, abnormal acquisition by the DUACS system can also lead to an abnormal data selection.

At this time, 5 altimeters constitute the altimeter constellation available in NRT.

- Jason-3 (J3) is the reference mission and also the oldest in the constellation.
- OSTM/Jason-2 interleaved: It does not present many events impacting the data availability. The last event for this platform occurred in December 2014, when the platform was in safe hold mode for a few days. Data were also missing for few days in October 2016 due to an orbit change manoeuver.
- SARAL-DP/AltiKa (AL). Few anomalies usually affect AltiKa data availability.
- Cryosat-2 (C2): This satellite presents more anomalies that Jason-2 or AltiKa. The last important event occurred during summer 2014, when a processing anomaly induced an important number of L2 missing measurements. These measurements were reprocessed afterward.

The Table 15 summarizes the main events affecting the data availability in NRT conditions..

Date	Platform	Event
2016/01/29	J2	AMR unavailable on 29/10/2015 from pass 17 at 05 :58 and until pass 20 at 08:26
2016/03/31	J2	AMR unavailable on 31/03/2016 from pass 85 at 09:30 and until pass 87 at 11:38
2016/04/05-06	J2	The OSTM/Jason-2 mission was interrupted from April, 5 (13h30 UTC) to April, 6 (12:00 UTC) to allow the upload of new GPS On Board software
2016/09 – 2016/10	C2	The L2 products were available with unusual delay during the period September-October 2016
2016/07/04-19	AL	Altika was deactivated from the DUACS processing during the mission orbit change maneuvers
2016/08/10-22	AL	Altika was deactivated from the DUACS processing due to algorithmic error linked to the important orbit drift
2016/09/12	J2	The OSTM/Jason-2 mission was deactivated in the system due to its change of orbit.
2016/09/12	J3	The Jason-3 mission was introduced in the NRT system
2016/11/14	J2N	The OSTM/Jason-2 interleaved mission was introduced in the system from November 14th 2016
2017/04/19	S3A	Sentinel-3A is introduced in DUACS processing

Table 15: Main events affecting the data availability in NRT conditions

V.3 Recent NRT sub-system evolutions overview

V.3.1 November 2016 – DUACS v16.1: Add OSTM/Jason-2 interleaved

The satellite OSTM/Jason-2 was moved on an interleaved orbit. The interleaved orbit is the same as that used for Jason-1 during the [mid-February 2009, March 2012] period: the new OSTM/Jason-2 ground track positions are midway between its original ground tracks but with a time lag of approximately 5 days with Jason-3. In other words, the start time of the OSTM/Jason-2 and Jason-3 repeat cycles will differ by approximately 5 days.

The orbit maneuvers started on October 2nd, at the end of the cycle 303 which is the last OSTM/Jason-2 cycle on the nominal ground track. The final interleaved orbit was reached on October 14th and the first cycle of measurement is numbered 305.

OSTM/Jason-2 interleaved has been reintroduced in the DUACS system in November 14th 2016, increasing the number of altimeters in the constellation. Up to 4 altimeters will be used in NRT processing with and additional “j2n” dataset corresponding to the OSTM/Jason-2 measurement on its interleaved orbit. **The measurement errors of OSTM/Jason-2 on its new orbit are the same as on its historical repeat orbit** (same as for Jason-3).

The Jason-3/OSTM-Jason-2 interleaved duo is optimized for mesoscale and circulation observation as previously discussed in Dibarboure et al (2011). This improved sampling will **contribute to improve the quality of the SLA gridded DUACS products (Level4 products)**.

V.3.2 November 2016 – DUACS v16.1: Change MSS solution used for geodetic/drifting missions processing

With this version, the DUACS has also changed the Mean Sea Surface (MSS) model involved in the SLA computation along geodetic or drifting orbits (Cryosat-2; SARAL-DP/AltiKa) for which no precise mean profile is available (see Pujol et al (2016) for details). The new MSS_CNES_CLS15 is now used instead of the previous MSS_CNES_CLS11 version. This change concerns the following regions/products: Global ocean, Europe, Mediterranean Sea and Black Sea.

The precision of the new MSS_CNES_CLS15 is strongly improved as underlined in Pujol et al (2015) and Schaeffer et al (2016). Figure 11 and Figure 12 illustrate this improvement:
Figure 11 shows that the SLA variance along HY-2A tracks confirmed the reduction of the MSS errors at wavelengths < ~250km with MSS_CNES_CLS_2015(note that HY-2A measurements are independent from all the MSS solutions).

- SLA Variance reduction along geodetic structures when comparing MSS_CNES_CLS_2015 with MSS_CNES_CLS_2011: locally more than 2 cm² at wavelengths [0, 250km]
- The comparison between MSS_CNES_CLS_2015 and MSS_DTU15 (other available MSS product) underlines:
    - Nearly the same capability of retrieving geodetic structures in both the MSS solutions.
    - A global SLA variance reduction at wavelengths [0, 250km] when using MSS_CNES_CLS_2015 rather than MSS_DTU15. This shows a more important commission errors and noises in MSS_DTU15.
    - A local SLA variance increase (e.g. Indonesian Sea) with MSS_CNES_CLS_2015 that highlight that some isolated structures are more accurate in MSS_DTU15.

Figure 12 underlines a significant improvement of the MSS_CNES_CLS_2015 solution in the Arctic region :

- Comparison of the SLA variance along Envisat tracks during the important melting ice that occurred in 2007 shows a significant reduction of the errors previously observed with MSS_CNES_CLS_11 in the Laptev Sea.
- Results obtained with MSS_CNES_CLS_2015 are comparable to results obtained with MSS_DTU15, with local exceptions that suggest that some isolated structures are more accurate in MSS_DTU15 (e.g. Foxe basin).

This MSS change improves the quality of the measurement along Cryosat-2; SARAL-DP/AltiKa tracks (Level3 products). The reduction of the errors on along-track products will also benefit to the SLA gridded products (Level4 products).

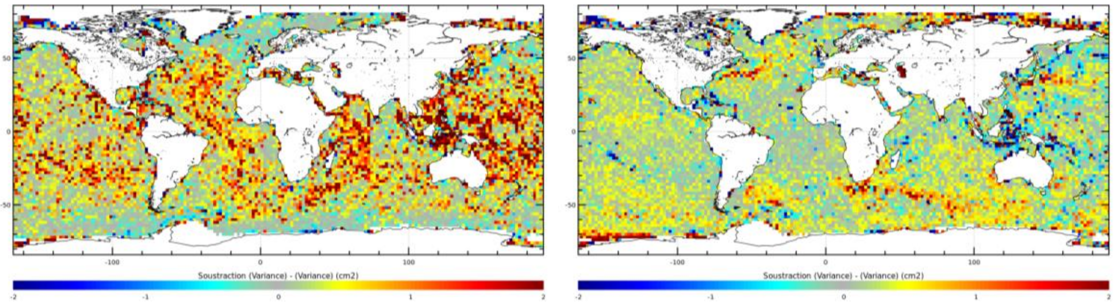

Figure 11: Right: Difference of the variance of the SLA selected on wavelength < 250km along HY-2A tracks when MSS_CNES_CLS_2011 and MSS_CNES_CLS_2015 is used. Statistics were computed over the year 2015. Left: same as right figure, but comparing SLA variance using MSS_CNES_DTU15 and MSS_CNES_CLS_2015 (plot range between -2 cm² (blue color) and +2 cm² (red color)).

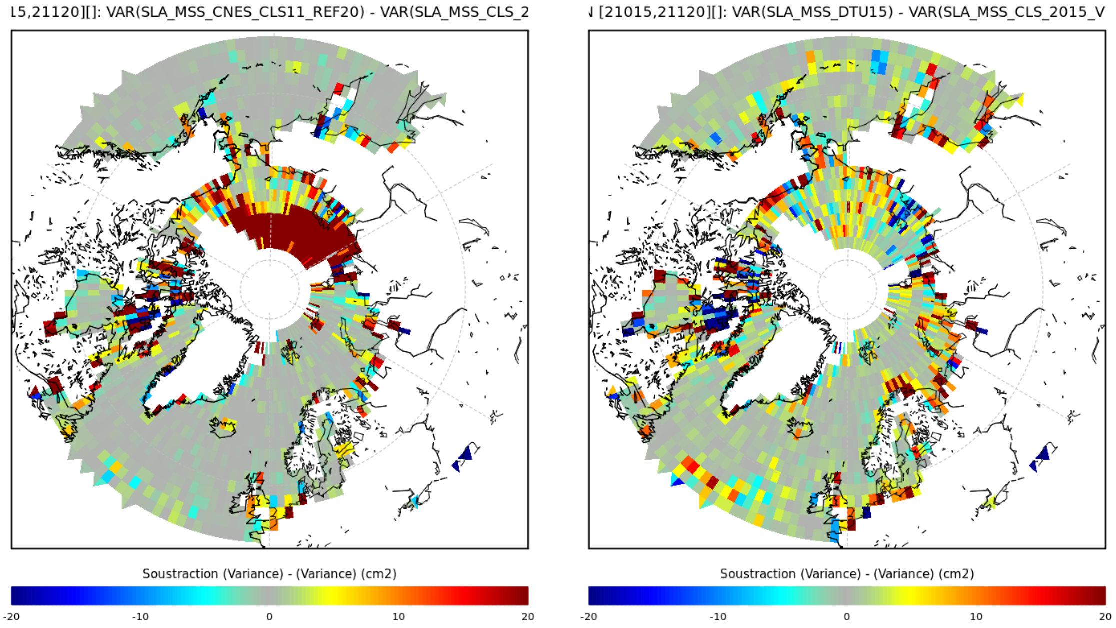

Figure 12: Right: Difference of the variance of the SLA along Envisat tracks when MSS_CNES_CLS_2011 and MSS_CNES_CLS_2015 is used. Statistics computed over [July, October 2007]. Left: same as right figure, but comparing SLA variance using MSS_CNES_DTU15 and MSS_CNES_CLS_2015.

V.3.3 April 2017 – DUACS v17.0: MSS solution changes for Arctic product

From April 19th 2017, the altimeter standards used in the Arctic region NRT processing is improved. The Mean Sea Surface (MSS) solution is indeed changed: the DTU13 (Andersen et al, 2015) field used in the previous version of the Arctic products is now replaced by the CNES_CLS15 version (Schaeffer et al, 2016). The improved quality of the CNES_CLS15, compared to the DTU13 and DTU15 is underlined by Pujol et al (2015) and Schaeffer et al (2016). It presents a reduced error at (sub-)mesoscale along the repetitive tracks (globally -0.75 cm rms for wavelengths ranging 0-200km along historical SARAL/AltiKa track) and equivalent error budget elsewhere.

The use of the MSS CNES_CLS15 over the Arctic region leads to an improved consistency between global and Arctic product. Figure 13illustrates the differences of SLA between the Global and Arctic products produced by the DUACS v17.0 version. They are globally lower than ±0.5 cm. Larger differences can be observed locally. They are induced by the different Mean Sea Surface or Mean Profile used for the Global and for the Arctic processing along Jason-2/3 tracks (see §II.4.6).Figure 14 shows the impact for the users at the transition between the previous and new Arctic product. The transition with previous product version leads to a SLA jump lower than nearly ±0.5 cm at latitude lower than 60°N. Elsewhere, SLA differences larger than 2 cm can be observed. They are characteristic of the differences observed between the MSS DTU13 and CNES_CLS15.

References:

Andersen O, P. A Knudsen, L. A Stenseng, The DTU13 MSS (Mean Sea Surface) and MDT (Mean Dynamic Topography) from 20 Years of Satellite Altimetry, International Association of Geodesy Symposia, 2015, http://dx.doi.org/10.1007/1345_2015_182

Pujol M.-I., Y. Faugere, G. Dibarboure, P Schaeffer, Amandine Guillot, N. Picot, The recent drift of SARAL:an unexpected MSS experiment. Presentation OSTST 2015, http://meetings.aviso.altimetry.fr/fileadmin/user_upload/tx_ausyclsseminar/files/OSTST2015/GEO-04-Pujol_OSTST2015.pdf

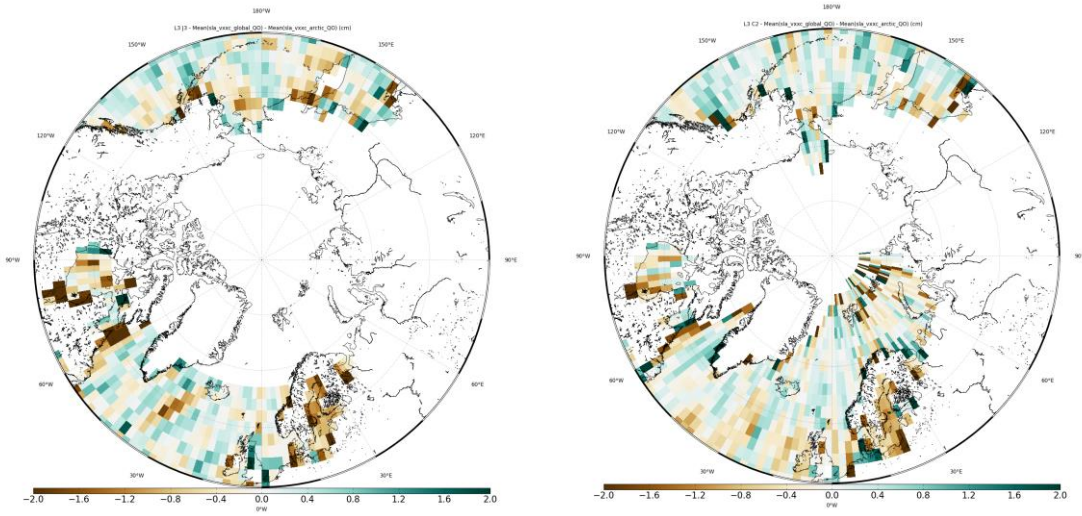

Figure 13: SLA differences between Global and Arctic L3 products produced by the new DUACS version. SLA measured along Jason-3 (left) and Cryosat-2 (right) tracks. Statistics were computed in 2°x2° boxes (units: cm)

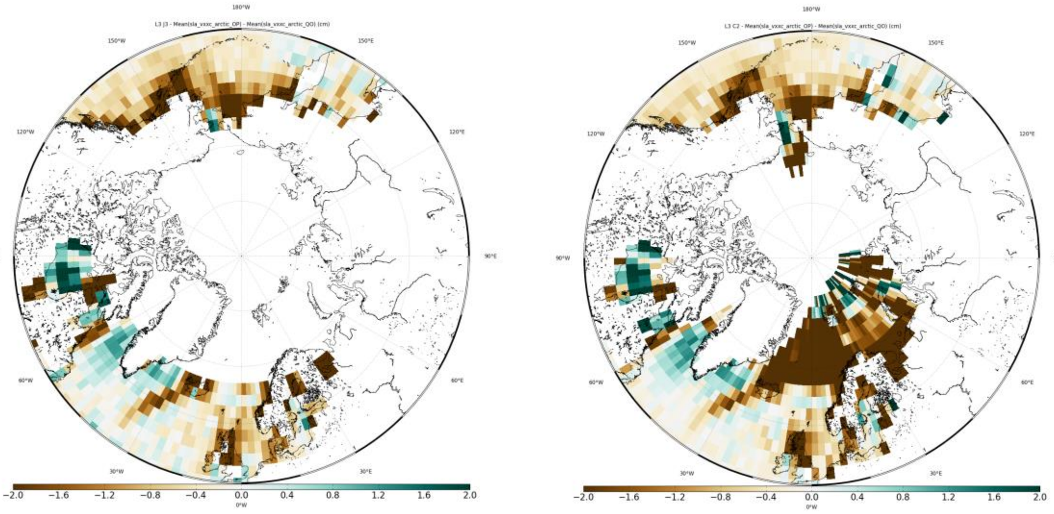

Figure 14: SLA differences between the previous and the new version of the Arctic L3 products. SLA measured along Jason-3 (left) and Cryosat-2 (right) tracks. Statistics were computed in 2°x2° boxes (units: cm)

V.3.4 April 2017 – DUACS v17.0: Sentinel-3A introduced in DUACS processing

The ESA (European Space Agency) mission Sentinel-3A was successfully launched in February 2016. From April 19th 2017, it is integrated in the DUACS NRT processing as a complementary mission and using L2p products from EUMETSAT.

Sentinel-3A is a multi-instrument mission to measure sea-surface topography, sea- and land-surface temperature, ocean colour and land colour with high-end accuracy and reliability. The mission will support ocean forecasting systems, as well as environmental and climate monitoring.

The SRAL (Sentinel Radar Altimeter) radar differs from previous conventional pulse limited altimeter in that it is capable of operating in several modes. The conventional or low resolution mode (LRM) was activated during the first cycle in order to ensure the continuity with the Synthetic Aperture Radar mode (SARM) activated since the 12th April 2016 over the global Ocean. The SARM (or Delay Doppler mode) full coverage is available for the first time in the altimetry history.

The Payload Data Ground Segment (PDGS) L2 Marine products release started on 13th of December 2016. The calibration and validation analyses performed highlighted the great quality of these products. The expected benefits bring by the Delay Doppler mode leading, among other, to a reduced instrumental white noise are well observed. The raw (i.e. not along-track low-pass filtered)SARM 1Hz level of noise at global scales is around 2.4 cm against 2.9 cm in LRM (for Sentinel-3A, Jason-2 and Jason-3). (see also §IV.1.1.2.1.).Moreover, using the spectral analysis, SLA comparison between Delay Doppler and conventional altimetry confirms that, as expected, the SARM mesoscales are not impacted by the bump error. Finally, cross comparison metrics ensure, at long wavelength, the consistency with respect to other altimeters.

To conclude, the available Sentinel-3A products constitute the first operational dataset including SARM at global scales. Despite of some aspects that should be improved, the dataset quality is already in line with expectations.

V.4 REP/DT sub-system version changes

System version	Date of the change	Description of the change
5.0	*January 2014*	Delayed-Time reprocessing
5.1	*June 2014*	Implementation of the constellation changes in the system :Integration of AltiKa
5.3	*October 2014*	Implementation of the constellation changes in the system Integration of HY-2A Production of the [May, June 2014] period
5.5	*February 2015*	Production of the [June, Oct. 2014] period
5.6	*May 2015*	Production of the [Nov., Dec. 2014] period
5.7	*November 2015*	Integration of the orbit standards change for Jason-2 from cycle 254 : correction of regional biases Change of the AltiKa processing to take into account the ground-track orbit drift during the period [April, August 2015] Production of the [Jan., April. 2015] period
5.7	*March 2016*	Production of the [May., Sept. 2015] period Change of the AltiKa processing to take into account the ground-track orbit drift during the period [April, August 2015]
5.7	*June 2016*	Production of the [Sept. 2015, mid January 2016] period Change of the AltiKa processing to take into account the ground-track orbit drift from October 2015 to July 4th 2016
5.7	*November 2016*	Production of the [mid January, April 2016] period
5.8	*April 2017*	Production of the [May, September 2016] period Altika moved to its geodetic orbit since 2016/07/04. Introduction of Jason-3 which replace Jason-2 (2016-06-25). Jason-3 is the new reference mission.
5.9	*June 2017*	Production of the [September, December 2016] period. Introduction of Sentinel-3A and Jason-2 Interleaved. Cryosat-2 upstream data change since cycle 88 for ESA GOP instead of CNES CPP. Six satellites are used in the DT processing chain (ALG, C2, H2, J2N, J3, S3A)

VI QUALITY CHANGES SINCE PREVIOUS VERSION

VI.1 REP processing

Differences between up-to-date REP dataset and previous version is fully discussed in Pujol et al. (2016), Capet et al (2015); Marcos et al (2015); Juza et al (2016). Main issues are given in the previous chapters.

VI.2 NRT processing

With DUACS v17.0, the quality of along-track products is mainly improved by the use of an up-to-date MSS over the Arctic region. The addition of Sentinel-3A altimeter in the constellation also contributes to improve the sea surface sampling over all the regions. This directly benefit to the gridded maps products quality, as discussed in §IV.1.2.3.

VII REFERENCES

Ablain M., Larnicol G., Faugere Y., Cazenave A., Meyssignac B., Picot N., Benveniste J., 2012, Error Characterization of Altimetry Measurements at Climate Scales, in Proceedings of the "20 Years of Progress in Radar Altimetry" Symposium, Venice, Italy, 24-29 September 2012, Benveniste, J. and Morrow, R., Eds., ESA Special Publication SP-710, 2012. DOI:10.5270/esa.sp-710.altimetry2012

Ablain, M. 2013. Validation Report: WP2500 Regional SSH Bias Corrections between Altimetry Missions. http://www.esa-sealevel-cci.org/Public Documents/SLCCI-ValidationReport_WP2500_AltimetrySSHBiasBetweenMissions.docx

M. Ablain, A. Cazenave, G. Larnicol, M. Balmaseda, P. Cipollini, Y. Faugère, M. J. Fernandes, O. Henry, J. A. Johannessen, P. Knudsen, O. Andersen, J. Legeais, B. Meyssignac, N. Picot, M. Roca, S. Rudenko, M. G. Scharffenberg, D. Stammer, G. Timms, and J. Benveniste, Improved sea level record over the satellite altimetry era (1993–2010) from the Climate Change Initiative project, Ocean Sci., 11, 67-82, doi:10.5194/os-11-67-2015, 2015

Arbic B. K, R. B. Scott, D. B. Chelton, J. G. Richman and J. F. Shriver: Effects on stencil width on surface ocean geostrophic velocity and vorticity estimation from gridded satellite altimeter data, J. Geophys. Res., vol 117, C03029, doi:10.1029/2011JC007367, 2012.

Aviso/SALP: Jason-2 validation and cross calibration activities (Annual report 2014) Jason-2 validation and cross calibration activities (Annual report 2014), edition 1.1, available at http://www.aviso.altimetry.fr/fileadmin/documents/calval/validation_report/J2/annual_report_j2_2014.pdf, last access 2016/03/31, 2015

Aviso/SALP, SARAL/AltiKa Products Handbook, edition 2.5, available at http://www.aviso.altimetry.fr/fileadmin/documents/data/tools/SARAL_Altika_products_handbook.pdf, last access 2017/01/10, 2016a

Aviso/SALP, OSTM/Jason-2 Products Handbook, edition 1.10, available at http://www.aviso.altimetry.fr/fileadmin/documents/data/tools/hdbk_j2.pdf, last access 2017/01/10, 2016b

Aviso/SALP, Jason-3 Products Handbook, edition 1.2, available at http://www.aviso.altimetry.fr/fileadmin/documents/data/tools/Shdbk_j3.pdf, last access 2017/01/10, 2016c

Aviso+, Along-track Level-2+ (L2P) Sentinel-3A Product Handbook, v1.2, 2016d (http://www.aviso.altimetry.fr/fileadmin/documents/data/tools/hdbk_L2P.pdf)

Boy F., J. D. Desjonquères, N. Picot, T. Moreau and M. Raynal, "CryoSat-2 SAR-Mode Over Oceans: Processing Methods, Global Assessment, and Benefits," in IEEE Transactions on Geoscience and Remote Sensing, vol. 55, no. 1, pp. 148-158, Jan. 2017.doi: 10.1109/TGRS.2016.2601958

Capet A., E. Mason, V. Ross, C. Troupin, Y. Faugere, M.-I. Pujol, A. Pascual: Implications of a Refined Description of Mesoscale Activity in the Eastern Boundary Upwelling Systems, Geophys. Res. Lett., 41, doi:10.1002/2014GL061770, 2014.

Carrère, L., andF. Lyard,Modeling the barotropic response of the global ocean to atmospheric wind and pressure forcing - comparisons with observations,Geophys. Res. Lett.,30, 1275, doi:10.1029/2002GL016473, 2003

Carrère, L, F. Lyard, M. Cancet, A. Guillot, N. Picot, 2015: FES2014: a new tidal model on the global ocean with enhanced accuracy in shallow seas and in the Arctic region, OSTST2015: http://meetings.aviso.altimetry.fr/fileadmin/user_upload/tx_ausyclsseminar/files/29Red1100-2_ppt_OSTST2014_FES2014_LC.pdf

Cartwright, D. E., R. J. Tayler: New computations of the tide-generating potential, Geophys. J. R. Astr. Soc., 23, 45-74, 1971

Cartwright, D. E., A. C. Edden: Corrected tables of tidal harmonics, Geophys. J. R. Astr. Soc., 33, 253-264, 1973

Chelton, D. B., Schlax, M. G., Samelson, R. M.: Global observationsof nonlinear mesoscale eddies, Prog. Oceanogr., 91, 167–216, doi:10.1016/j.pocean.2011.01.002, 2011.

Chelton D., G. Dibarboure , M.-I. Pujol, G. Taburet , M. G. Schlax: The Spatial Resolution of AVISO Gridded Sea Surface Height Fields, OSTST Lake Constance, Germany, October, 28-31 2014, available at http://meetings.aviso.altimetry.fr/fileadmin/user_upload/tx_ausyclsseminar/files/29Red0900-1_OSTST_Chelton.pdf, 2014

Couhert A.; L. Cerri; JF Legeais; M. Ablain; N. Zelensky; B. Haines; F. Lemoine; W. Bertiger; S. Desai; M. Otten; Towards the 1 mm/y Stability of the Radial Orbit Error at Regional Scales. Advances in Space Research, 2014. doi:10.1016/j.asr.2014.06.041

Dibarboure G., M-I. Pujol, F. Briol, P.-Y. Le Traon, G. Larnicol, N. Picot, F. Mertz, P. Escudier , M. Ablain, and C. Dufau: Jason-2 in DUACS: first tandem results and impact on processing and products, Mar. Geod., OSTM Jason-2 Calibration/Validation Special Edition – Part 2, (34), 214-241, doi:10.1080/01490419.2011.584826, 2011

Dibarboure, G., F. Boy, J.D. Desjonqueres, S. Labroue, Y. Lasne, N. Picot, J.C. Poisson and P.Thibaut: Investigating Short-Wavelength Correlated Errors on Low-Resolution Mode Altimetry, *J. Atmospheric Ocean. Technol.*, 31, 1337–1362. doi:10.1175/JTECH-D-13-00081.1, 2014

Ducet N., P.-Y Le Traon., G. Reverdun: Global high-resolution mapping of ocean circulation from TOPEX/Poseidon and ERS-1 and -2, J. Geophys. Res. 105 (C8), 19,477-19,498, 2000

Dufau, C., Orstynowicz, M., Dibarboure, G., Morrow, R., and La Traon, P.-Y.: Mesoscale Resolution Capability of altimetry: present & future, J. Geophys. Res, 121, 4910–4927, doi:10.1002/2015JC010904, 2016.

Juza, M., Escudier, R., Pascual, A., Pujol, M.-I., Taburet, G., Troupin, C., Mourre, B., and Tintoré, J.: Impacts of reprocessed altimetry on the surface circulation and variability of the Western Alboran Gyre, Adv. Space Res., 58, 277–288, doi:10.1016/j.asr.2016.05.026, 2016.

Lagerloef, G.S.E., G.Mitchum, R.Lukas and P.Niiler: Tropical Pacific near-surface currents estimated from altimeter, wind and drifter data,J. Geophys. Res., 104, 23,313-23,32, 1999

Legeais J.-F., M. Ablain and S. Thao. Evaluation of wet troposphere path delays from atmospheric reanalyses and radiometers and their impact on the altimeter sea level. Ocean Science, 10, 893-905, 2014. doi: 10.5194/os-10-893-2014. http://www.ocean-sci.net/10/893/2014/os-10-893-2014.pdf

Le Traon, P.-Y., and F. Ogor: ERS-1/2 orbit improvement using TOPEX/POSEIDON: The 2 cm challenge. J. Geophys. Res., 103, 8045–8057, 1998.

Le Traon P.-Y., F. Nadal, N. Ducet, An Improved Mapping Method of Multisatellite Altimeter Data, ?, J. Atmos. Oceanic Technol. 15, 522-534, 1998

LeTraon P.-Y, Y. Faugere, F. Hernamdez, J. Dorandeu, F. Mertz and M. Abalin: Can We Merge GEOSAT Follow-On with TOPEX/Poseidon and ERS-2 for an Improved Description of the Ocean Circulation?, J. Atmos. Oceanic Technol., 20, 889-895, 2003

Marcos M., Pascual, A., and Pujol, M.-I.: Improved satellite altimeter mapped sea level anomalies in the Mediterranean Sea: A comparison with tide gauges, Adv. Space Res., 56, 596–604, doi:10.1016/j.asr.2015.04.027, 2015.

Mulet, S., Rio, M. H., Greiner, E., Picot, N., and Pascual, A.: New global Mean Dynamic Topography from a GOCE geoid model, altimeter measurements and oceanographic in-situ data, OSTST Boulder USA 2013, available at: http://www.aviso.altimetry.fr/fileadmin/documents/OSTST/2013/oral/mulet_MDT_CNES_CLS13.pdf (last access: 31 August 2016), 2013.

Pascual, A., Faugere, Y., Larnicol, G., and Le Traon, P.-Y.: Improved description of the ocean mesoscale variability by combining four satellite altimeters, Geophys. Res. Lett., 33, L02611, doi:10.1029/2005GL024633, 2006.

Pascual A., C Boone, G Larnicol, P-YvLe Traon, 2008, On the Quality of Real-Time Altimeter Gridded Fields: Comparison with In Situ Data, J. Atmosph. and Ocean. Techno., 26, 556–569

Prandi, P., B. Meyssignac, M. Ablain and L. Zawadzki. How reliable are regional sea level trends from satellite altimetry? In preparation.

Pujol, M.-I., Faugère, Y., Taburet, G., Dupuy, S., Pelloquin, C., Ablain, M., and Picot, N.: DUACS DT2014: the new multi-mission altimeter data set reprocessed over 20 years, Ocean Sci., 12, 1067-1090, doi:10.5194/os-12-1067-2016, 2016

Ray R.D. and Zaron E.D.: M2 internal tides and their observed wavenumber spectra from satellite altimetry, J. Phys. Oceanogr., 46, doi: 10.1175/JPO-D-15-0065.1, 2015.

Rio M.-H , S. Mulet and N. Picot, 2014a. Beyond GOCE for the ocean circulation estimate: Synergetic use of altimetry, gravimetry and in-situ data provides new insight into geostrophic and Ekman currents. GRL.

Rio, M.-H., Pascual, A., Poulain, P.-M., Menna, M., Barceló, B., and Tintoré, J. (2014b). Computation of a new mean dynamic topography for the Mediterranean Sea from model outputs, altimeter measurements and oceanographic in situ data. Ocean Sci., 10, 731-744, doi:10.5194/os-10-731-2014.

Scharro R., J. Lillibridge, S. Abdalla, D. Vandemark, Early look at SARAL/AltiKa data. Presentation at OSTST 2013. Available at http://www.aviso.altimetry.fr/fileadmin/documents/OSTST/2013/oral/Scharroo_Early_look_at_SARAL.pdf (last access January 10th 2016).

Schaeffer P., I. Pujol, Y. Faugere, A. Guillot, N. Picot, The CNES CLS 2015 Global Mean Sea surface.Presentation OSTST 2016, http://meetings.aviso.altimetry.fr/fileadmin/user_upload/tx_ausyclsseminar/files/GEO_03_Pres_OSTST2016_MSS_CNES_CLS2015_V1_16h55.pdf (last access 2017/01/10)

SL_cci Comprehensive Error Characterization Report, CLS-DOS-NT-13-100, SLCCI-ErrorReport-030-2-2, Jul. 29,2016, http://www.esa-sealevel-cci.org/webfm_send/537

Tran N., S. Philipps, J.-C. Poisson, S. Urien, E. Bronner, N. Picot, "Impact of GDR_D standards on SSB corrections", Presentation OSTST2012 in Venice, http://www.aviso.altimetry.fr/fileadmin/documents/OSTST/2012/oral/02_friday_28/01_instr_processing_I/01_IP1_Tran.pdf, 2012

Wahr, J. W.: Deformation of the Earth induced by polar motion, ,J. Geophys. Res. (Solid Earth), 90, 9363-9368, 1985

Zawadzki L. and Ablain M. 2015. Accuracy of the mean sea level continuous record with future altimetric missions: Jason-3 versus Sentinel-3a. Submitted to Ocean Science. In revision.